

Project

Design of a Modern Passenger Aircraft with Diesel Engine and Propeller

Author: Tobias Albrecht

Supervisor: Prof. Dr.-Ing. Dieter Scholz, MSME
Submitted: 2023-10-07

Faculty of Engineering and Computer Science
Department of Automotive and Aeronautical Engineering

DOI:

<https://doi.org/10.15488/xxxxx>

URN

<https://nbn-resolving.org/urn:nbn:de:gbv:18302-aero2023-10-07.018>

Associated URLs:

<https://nbn-resolving.org/html/urn:nbn:de:gbv:18302-aero2023-10-07.018>

© This work is protected by copyright

The work is licensed under a Creative Commons Attribution-NonCommercial-ShareAlike 4.0 International License: CC BY-NC-SA

<http://creativecommons.org/licenses/by-nc-sa/4.0>



Any further request may be directed to:

Prof. Dr.-Ing. Dieter Scholz, MSME

E-Mail see: <http://www.ProfScholz.de>

This work is part of:

Digital Library - Projects & Theses - Prof. Dr. Scholz

<http://library.ProfScholz.de>

Published by

Aircraft Design and Systems Group (AERO)

Department of Automotive and Aeronautical Engineering

Hamburg University of Applied Science

This report is deposited and archived:

- Deutsche Nationalbibliothek (<https://www.dnb.de>)
- Repository of Leibniz University Hannover (<https://www.repo.uni-hannover.de>)
- Internet Archive (<https://archive.org>)
Item: <https://archive.org/details/TextAlbrecht.pdf>

This report has associated published data in Harvard Dataverse:

<https://doi.org/10.7910/DVN/VQCSCF>

Abstract

Purpose – This project investigates the economic viability of a large diesel-powered passenger aircraft based on the Airbus A320-200 Top Level Aircraft Requirements (TLAR) and its possible contribution to reducing CO₂ emissions.

Methodology – A redesign of the A320-200 is used as reference aircraft. In a second step, a turboprop aircraft that meets the previously defined requirements is prepared. The difference is just in the engines and the cruise Mach number reduced from 0.78 to 0.68. In a third step, an aircraft with diesel engines and propellers is sized. The required parameters for this engine are determined from literature. In addition, a possible use of the diesel aircraft for a shorter flight distance is examined. Preliminary sizing is done with existing spreadsheets adapted to diesel engine parameters.

Findings – The power-specific fuel consumption of the turboprop and the diesel aircraft were both set to 210 g/kWh. While the maximum take-off mass of the turboprop aircraft is only 2% higher than that of the turbofan aircraft, it is as much as 84% higher for the diesel aircraft. This is due to the low power density of the diesel aircraft, which is just 1 kW/kg, while being 4.15 kW/kg for the turboprop. As a result, the turboprop only consumes 3.5% more fuel than the turbofan, while the diesel aircraft consumes about 87% more fuel than the turbofan. With range reduced from 2125 NM to 500 NM, maximum take-off mass and fuel mass increase is less, but still very high for the diesel aircraft. Therefore, it is not possible to use large passenger diesel aircraft in an economically or ecologically reasonable way.

Research limitations – Work is done on preliminary sizing level.

Practical implications – The existing preliminary sizing tools for turboprop aircraft can now also be used for the calculation of aircraft with piston engines.

Social implications – A comparison of large passenger aircraft with turbofan, turboprop, and diesel aircraft is now possible. This allows a fact-based discussion about a possible use of diesel engines for large passenger aircraft.

Originality – A comparison of engine options for large passenger aircraft including diesel engines could not be found in the literature. It is now part of the scientific body of knowledge.

Design of a Modern Passenger Aircraft with Diesel Engine and Propeller

Task for a *Project* (Master studies)

Background

Starting point for this project is the [TV Documentary](#) from 2022 and the related [Press Release](#) by Steinhausen and Scholz titled "Flying with Diesel Engine and Propeller". Accordingly, diesel engines may have a higher efficiency than other engine types. Propeller aircraft benefit from their high propulsive efficiency. Drag of propeller aircraft may be lower due to their lower cruise speed. Lower fuel burn and lower flight altitude may lead to lower equivalent CO₂ emissions. Nevertheless, diesel engines with propeller may not be better than turbofans, when their overall efficiency is compared ([Mahfouz 2023](#)). Part of the comparison with conventional passenger jets are also maintenance costs and the purchase price (which determines depreciation). Diesel engines are in use and have been used in aviation before. As such, their introduction should cause less problems than other proposed new technologies based e. g. on hydrogen or batteries. Much information is available to solve the task: A redesign of the Airbus A320 as well as various Excel tables for preliminary sizing and optimization of jet and propeller driven passenger aircraft.

Task

Based on the Top Level Aircraft Requirements (TLARs) of the A320 or A320neo a turboprop aircraft should be designed and in a second step an aircraft with diesel engines and propeller. The following subtasks should be considered:

- Short review and background: Diesel engines and propellers.
- Redesign of the A320 (turbofan engines).
- Preliminary sizing of an aircraft with A320 TLARs with turboprop engines.
- Preliminary sizing of an aircraft with A320 TLARs with diesel engine and propellers.
- Comparison of the three aircraft designs.
- Preliminary sizing of all three aircraft with reduced range.
- Discussion of the results and evaluation of the diesel concept.

The report has to be written in English based on German or international standards on report writing.

Table of Contents

	Page
List of Figures	6
List of Tables.....	7
List of Symbols	8
List of Abbreviations.....	11
1 Introduction	12
1.1 Motivation	12
1.2 Title Terminology.....	12
1.3 Task	13
1.4 Literature Review	14
1.5 Structure	15
2 State of the Art.....	16
2.1 Diesel Engines in Aviation.....	16
2.2 Aircraft Propellers	17
2.3 Aircraft with Diesel Engines and Propeller.....	19
2.3.1 Use in Light Aircraft	19
2.3.2 Otto Aviation Celera 500L	20
3 Preliminary Sizing.....	21
3.1 A320 with Turbofan (Reference Aircraft).....	21
3.2 A320 with Turboprop.....	27
3.3 A320 with Diesel Engine	35
4 Preliminary Sizing for Shorter Range.....	39
4.1 A320 with Turbofan	39
4.2 A320 with Turboprop.....	42
4.3 A320 with Diesel Engine	44
5 Summary	47
6 Conclusions and Recommendations	48
List of References	49
Appendix A – Input Parameter Long Range.....	55
Appendix B - Input Parameter Short Range.....	58

List of Figures

Figure 2.1	RED A03 engine	17
Figure 2.2	Airbus A400M 8-blade propeller	18
Figure 2.3	DA40 NG	19
Figure 2.4	Otto Aviation Celera 500L.....	20
Figure 3.1	Runway length take-off.....	22
Figure 3.2	Landing field length.....	22
Figure 3.3	Payload-range diagram	23
Figure 3.4	Maximum glide ratio.....	24
Figure 3.5	Matching Chart turbofan aircraft	25
Figure 3.6	Matching Chart turboprop aircraft.....	28
Figure 3.7	Matching Chart diesel aircraft	35
Figure 4.1	Matching Chart turbofan aircraft (500 NM)	41
Figure 4.2	Matching Chart turboprop aircraft (500 NM).....	42
Figure 4.3	Matching Chart diesel aircraft (500 NM)	46

List of Tables

Table 3.1	Reference data Airbus A320-200 WV017	21
Table 3.2	Output data Excel tool turbofan aircraft	26
Table 3.3	System masses turbofan aircraft	29
Table 3.4	System masses turboprop aircraft	32
Table 3.5	Output data Excel tool turboprop aircraft	33
Table 3.6	System masses diesel aircraft.....	37
Table 3.7	Mass comparison of all three engine types	38
Table 4.1	System masses turbofan aircraft (500 NM)	40
Table 4.2	Output data Excel tool turbofan aircraft (500 NM)	41
Table 4.3	System masses turboprop aircraft (500 NM)	43
Table 4.4	Output data Excel tool turboprop aircraft (500 NM)	44
Table 4.5	System masses diesel aircraft (500 NM)	45
Table 4.6	Mass comparison of all three engine types (500 NM).....	46
Table A.1	Input data Excel tool turbofan aircraft	55
Table A.2	Input data Excel tool turboprop aircraft.....	56
Table A.3	Input data Excel tool diesel aircraft	57
Table B.1	Input data Excel tool turbofan aircraft (500 NM).....	58
Table B.2	Input data Excel tool turboprop aircraft (500 NM).....	59
Table B.3	Input data Excel tool diesel aircraft (500 NM)	60

List of Symbols

A	Aspect ratio
b	Wing span
C	Coefficient
c	Specific fuel consumption
C_D	Drag coefficient
C_L	Lift coefficient
d	Diameter
e	Span efficiency factor (Oswald Factor)
E	Glide ratio L/D
g	Earth acceleration
k	Constant
M	Mach number
m	Mass
M_{ff}	Mission fuel fraction
m/S_W	Wing loading
n	Indicates the number of elements
P	Power
$P/(m \cdot g)$	Power-to-weight ratio
pd	Power density
R	Range
s	Distance
S_W	Wing surface area
T	Thrust/ Temperature
$T/(m \cdot g)$	Thrust-to-weight ratio
V	Velocity

Greek Symbols

η	Efficiency
λ_{BPR}	Bypass ratio (BPR)
σ	Density ratio

Indices

Indices for flight phases

<i>APP</i>	Approach
<i>CLB</i>	Climb
<i>CR</i>	Cruise
<i>DES</i>	Descent
<i>L</i>	Landing
<i>MA</i>	Missed Approach
<i>T</i>	Taxi
<i>TO</i>	Take-off

Indices for Aircraft Components

<i>E</i>	Engine
<i>H</i>	Horizontal tailplane
<i>NA</i>	Nacelle
<i>P</i>	Propeller
<i>PY</i>	Pylon
<i>UC</i>	Undercarriage
<i>TR</i>	Thrust reverser
<i>V</i>	Vertical tailplane
<i>W</i>	Wing

Other Indices

<i>alternate</i>	Flight distance to alternate airport
<i>BPR</i>	Bypass ratio
<i>C</i>	Crew
<i>cargo</i>	Cargo
<i>D</i>	Diesel aircraft
<i>D, 0</i>	Zero lift drag
<i>D, slat</i>	Drag induced by the slats
<i>DEP</i>	Depreciation
<i>disc</i>	Disc
<i>F</i>	Fuel
<i>FEE</i>	Fees and charges
<i>INT</i>	Interest

<i>INS</i>	Insurance
<i>LFL</i>	Landing field length
<i>LR</i>	Long range
<i>M</i>	Maintenance
<i>max</i>	Maximum
<i>md</i>	Minimum drag
<i>ME</i>	Maximum empty
<i>ML</i>	Maximum landing
<i>MR</i>	Maximum ramp
<i>MTO</i>	Maximum take-off
<i>MZF</i>	Maximum zero fuel
<i>OE</i>	Operating empty
<i>PAX</i>	Passengers, PAX
<i>PL</i>	Payload
<i>PSFC</i>	Power specific fuel consumption
<i>SR</i>	Short range
<i>TF</i>	Turbofan
<i>TP</i>	Turboprop aircraft
<i>TP400 – D6</i>	TP400-D6 turbofan engine
<i>TSFC</i>	Thrust specific fuel consumption
<i>TOFL</i>	Take-off field length

List of Abbreviations

A/C	Aircraft
BPR	Bypass Ratio
CFK	Carbon Fiber Reinforced Plastic
CFRTP	Carbon Fiber Reinforced Thermoplastic
CS	Certification Specifications
DIFF	Difference
DOC	Direct Operating Costs
EASA	European Union Aviation Safety Agency
ECS	Environmental Control System
FAR	Federal Aviation Regulations
hydr. /pneu. Sys.	Hydraulic/ Pneumatic System
IAE	International Aero Engines
ISA	International Standard Atmosphere
ISBN	International Standard Book Number
MS	Microsoft
PDF	Portable Document Format
PreSTo	Preliminary Sizing Tool
PSFC	Power-Specific Fuel Consumption
RED	Raikhlin Aircraft Engine Developments
SAF	Sustainable Aviation Fuels
TSFC	Thrust-Specific Fuel Consumption
URL	Universal Resource Locator
WV	Weight Variant
WWW	World Wide Web

1 Introduction

1.1 Motivation

This project deals with the preliminary sizing of an aircraft with diesel engines. The background is a short tv broadcast of Steinhausen (2022) from 3sat about diesel engines and its possibility to improve the environmental impact in the aerospace sector. With Prof. Dr. Dieter Scholz as an expert, different older technologies were shown with their potential for aircraft designs of today. For example, the Douglas DC-6, which is still in service, or a small manufacturer in Adenau, which produces diesel engines for mostly two-seater training aircraft. But already in the 50's and 60's piston engines were used in aircraft that were able to cross the Atlantic with up to 105 people on board. Given the high efficiency of diesel piston engines and their price advantage over jet engines, the question is whether it makes sense to revive them for large commercial aircraft like the A320. In addition, the diesel engine is capable of running on synthetic fuels and even conversion to hydrogen would be possible. Thanks to turbocharging, the diesel engine is highly efficient at any altitude and with the use of catalysts, air pollution can be significantly reduced (Steinhausen 2022). This raises the question why this technology, despite its many advantages, is not receiving more attention in today's aeronautics research, even though it can contribute a great deal to making aviation more environmentally friendly. Getting to the bottom of this question is the motivation for this thesis.

1.2 Title Terminology

In this chapter, the title of this thesis is broken down into its parts and explained piece by piece. The title of this project is “Design of a Modern Passenger Aircraft with Diesel Engine and Propeller”. First, the term *design* in the context of aircraft design reflects the actual task very well. Then the aircraft to be designed is defined as a *modern passenger aircraft*. This is further specified by the mentioned components *diesel engine* and *propeller*.

Design

„*Design*: Creating the geometric description of a thing to be built.” (Raymer 2018)

Modern

Modern can be described as “(...) existing in the present or a recent time, or using or based on recently developed ideas, methods, or styles: (...)” (Cambridge 2023)

Passenger Aircraft

“Passenger is used to describe something that is designed for passengers, rather than for drivers or goods.” (Collins 2023a)

“An aircraft is a vehicle which can fly, for example an aeroplane or a helicopter.” (Collins 2023b)

Diesel Engine

“A diesel engine is an internal combustion engine in which oil is burnt by very hot air.” (Collins 2023c)

Propeller

“A propeller is a device with blades which is attached to a boat or aircraft. The engine makes the propeller spin round and causes the boat or aircraft to move.” (Collins 2023d)

1.3 Task

The aim of this work is to evaluate the suitability of a diesel piston engine as a propulsion system for an aircraft of the size of the Airbus A320. This includes a comparison of a diesel aircraft with a turboprop and a turbofan aircraft based on the A320-200.

The first step is to research and present the fundamental facts about the diesel engine and the propeller. The top-level requirements on which the design is based are then researched and verified by redesigning the A320 as a turbofan. In the next step, these can be used to design a turboprop aircraft. Since the individual configurations are fundamentally different, the differences must be clearly defined and the relevant modifications and performance parameters investigated. By making further adjustments, the diesel aircraft can be sized on the basis of the turboprop aircraft and compared with the others. In a further step, the range requirement is changed to show the performance of each aircraft under these new conditions.

1.4 Literature Review

There is limited literature on diesel-powered piston engines in aircraft design within the past 20 years. In particular, nothing can be found on the use in aircraft that fall under the CS-25 certification regulation.

Therefore, there are publications on piston engines in small aircraft or drones. These primarily provide reference values for power density and power-specific fuel consumption. In addition, general information on the use of 2-stroke or 4-stroke engines as well as advantages over jet engines is provided. This literature includes publications by Cantore (2014), Carlucci (2015 and 2016), Grabowski (2017), Grabowski (2019) and Xu (2021).

Many of the key data were obtained from a product data sheet of the RED A03 engine from Raikhlin Aircraft Engine Developments (RED Aircraft 2023). In addition, further information could be obtained during a visit to the factory in a personal conversation with one of the employees Sebastian Quink. Sebastian Quink mainly provided information on the purchase price, the maintenance process, including maintenance intervals and maintenance requirements, as well as current and future applications of the diesel engine.

The top-level requirements for dimensioning can be found in the Airbus A320-200 product data sheet (Airbus 1985). In addition, this document contains many diagrams that can be used to evaluate the plausibility of the redesign.

Other reference values can be obtained from product data sheets. In addition to values for the engine of the reference aircraft, these also include data for the turboprop aircraft. The values are taken from Austro Engine (2022), EASA (2015b and 2023), MTU (2023) and Technify Motors (2014).

For the redesign of the turbofan aircraft, a Microsoft (MS) Excel tool developed by Scholz (2023), Professor at the University of Applied Sciences Hamburg, Department of Automotive and Aeronautical Engineering, is used.

For the sizing of a turboprop aircraft, the Excel tool of Krull (2022) is used. This is a derivative of the tool of Dieter Scholz mentioned before. In addition, the work of Niță (2008 and 2013), Sánchez Barreda (2013) and Scholz (2009), as well as the lecture notes of Scholz (2015) and Braun (2020) serve as a further basis for the design of the turboprop configuration. The comparison of each aircraft is performed with the help of the work on the comparison of turboprop and turbofan by Mahfouz (2023).

Additional background information is obtained from the publications within the framework of Airport2030 by Johanning (2012, 2013 and 2014) and Scholz (2014).

1.5 Structure

The report is structured in six main chapters.

- Chapter 2** cites previous work covering general facts about diesel engines, propellers and existing aircraft with a combination of the two.
- Chapter 3** deals with the preliminary sizing of all three aircraft with a range of 2125 NM and discusses the main differences.
- Chapter 4** deals with the preliminary sizing of all three aircraft with the shorter range of 500 NM and discusses the main differences.
- Chapter 5** gives a summary of the preliminary sizings done with both ranges.
- Chapter 6** gives a conclusion of the previous chapters and gives recommendations for future work.
- Appendix A** shows an overview of all input parameters of the three different aircraft with a range of 2125 NM (Chapter 3).
- Appendix B** shows an overview of all input parameters of the three different aircraft with a range of 500 NM (Chapter 4).

The corresponding Excel tables of the Chapters 3 and 4 are stored in Harvard Dataverse:

<https://doi.org/10.7910/DVN/VQCSCF>

2 State of the Art

This chapter describes the state of the art of diesel engines in aviation. It begins with the diesel engine itself and its advantages and disadvantages compared to jet engines. The next chapter discusses the characteristics of propellers, which convert the shaft power of the diesel engine into propulsive power. This is followed by a presentation of the practical use of this combination in various aircraft.

2.1 Diesel Engines in Aviation

Diesel-powered piston engines in aviation are primarily used in small aircraft. In the mid-1950s, however, AvGas-fueled piston engines were also used in large aircraft such as the DC-7, where they were replaced by jet engines (Boyne 2006). Well-known engines are the Wright R-3350 or the Pratt & Whitney R-4360 (Boyne 2000). The reason for their replacement was the higher efficiency of jet engines, especially at high speeds, as well as their higher power density and therefore higher power-to-weight ratio. On the other hand, the advantages of diesel piston engines are their robustness and much simpler technology. They require less maintenance and have a longer service life. Only one oil change is required every 1000 flight hours (Quink 2022). The purchase price for small engines such as the RED A03 is \$170000 for 368 kW of power (Quink 2022). However, this is a low-volume engine, so lower prices would be expected if the engine were produced in high volume.

The differences between aircraft and automotive piston engines are due to special safety requirements and more extreme accelerations caused by flight maneuvers. For example, two separate ignition systems are required to ensure a certain power output even if one system fails. In addition, aircraft piston engines are air-cooled because it is lighter than liquid cooling and cannot fail due to leakage during flight (Grabowski 2017). Another major difference is the use of 2-stroke engines, which have a higher power density than the 4-stroke engines used in cars and operate at a lower crankshaft speed, allowing the engine to be connected to the propeller without a gearbox. (Cantore 2014, Carlucci 2016, Grabowski 2019, Xu 2021)

The power densities of diesel piston engines vary from 0.6 kW/kg to 1 kW/kg (Cantore 2014). The RED A03-003 engine from Raikhlin Aircraft Engine Developments (see Figure 2.1) delivers 368 kW at a mass of 363 kg (RED Aircraft 2023). This includes the complete control electronics as well as the control for the optimized propeller pitch angle (Quink 2022). In this paper a power density of 1 KW/kg is used for the calculation.



Figure 2.1 RED A03 engine

The power specific fuel consumption is in the range of 200 g/kWh and 240 g/kWh (Cantore 2014; Grabowski 2017; Grabowski 2019). For this project, the value chosen is that of the RED A03 engine, which is 210 g/kWh (Quink 2022).

2.2 Aircraft Propellers

The propeller provides the frictional connection between the engine and the air. It converts the mechanical shaft power of the engine into propulsive power. This is accomplished by the propeller blades, which are shaped like a wing profile. Unlike a wing profile, the shape is not constant over the entire blade length, but changes. This is because, as the propeller rotates, the flow speeds on the outside of the blade are higher than on the inside, requiring different angles of attack. (Mises 1933)

Most propellers are variable pitch. The angle of attack of the propeller blades can be adjusted to suit different flight conditions. During take-off and climb, a higher angle of attack can increase thrust, resulting in a lower engine load and therefore lower fuel consumption. The propeller can also provide reverse thrust for landing and ground maneuvering. In the event of an in-flight engine failure, the propeller blades are moved to the sail position to reduce drag and improve glide ratio. A disadvantage of a controllable pitch propeller is the increased maintenance and inspection requirements. Blade pitch control is usually hydraulic or electric. In addition, some aircraft have a propeller gearbox to adjust the engine speed to the optimum propeller speed. (Lage 2022)

Unlike an airfoil, the propeller generates centrifugal forces as it rotates, causing the air particles of the attached flow to be thrown outward. The attached boundary layer becomes thinner and

more dynamic and breaks off later at higher angles of attack and therefore higher forces. At optimum speeds, a fixed-pitch propeller can achieve efficiencies of up to 90% and is significantly more efficient than a jet engine. However, the jet engine provides greater acceleration and a more streamlined positioning of the airflow, resulting in higher airspeeds. With a propeller, the front of the attached motor is in the airflow. This is where electric motors have an advantage over piston engines because of their compactness. The maximum economically viable speed of a propeller-driven aircraft is about 700 km/h. (Hansen 2021, Lage 2022)

The limiting factor for the size of the propeller blades and the speed of the propeller is the blade tip speed. This speed must be lower than the speed of sound, otherwise flow separation due to sound waves can occur. In addition, the local flow around the airfoil further increases the flow velocity. To generate the required propulsive force, the number of propeller blades can be increased. This also reduces noise. Typically, propellers have at least two blades, but with the addition of a counterweight, single-blade propellers can be realized (Hansen 2021). An example of an engine with many blades is the A400M. The four TP400-D6 engines have eight blades each, with a blade length of about 5 m (Figure 2.2) (MTU 2023).



Figure 2.2 Airbus A400M 8-blade propeller (MTU 2023)

The three main materials used for propellers are wood, metal, and structural composites. The first propellers were made of wood over 100 years ago, and wooden propellers are still in use today. Today's wood propellers are made of natural composites with a highly compressed, glue-impregnated wood core that is bonded together from many individual layers of wood. The core is then covered with a layer of plastic. The advantage of wood is its light weight, which is half that of a metal propeller. This reduces the moment of inertia and, in addition to the natural damping of the wood, results in a smoother rotation, which prevents the occurrence of fatigue

fractures at the blade tips. Metal propellers are more commonly used on large aircraft and are more robust than wooden propellers. In addition, the higher strength allows for slimmer and thinner blades, which improves efficiency. Structural composite propellers have a plastic core and an outer skin of composite material, often carbon fiber reinforced thermoplastic (CFRTP). The composite material provides the structural function. Advantages include low weight and the ability to create a variety of blade shapes. This provides aerodynamic benefits. The leading edge of structural composite propellers is protected from damage by a metal strip. (Lage 2022)

2.3 Aircraft with Diesel Engines and Propeller

The first aircraft diesel engines were produced in the late 1920s and 1930s. One of the most famous was the Jumo 205 used in the German Junkers Ju 86 monoplane bomber (Cantore 2014). However, the diesel engine never really entered the market until recently. Now they are mainly used in various light aircraft. In the future, they will also be used to power a six-seat business jet.

2.3.1 Use in Light Aircraft

The use of diesel engines in light aircraft continues to grow. This is because direct injection and turbocharging provide power densities that make them suitable for use in light aircraft. The advantage over gasoline engines is their low fuel consumption. The CD-135 diesel engine from Technify Motors, also known under its former name Centurion 1.7, is a 4-cylinder in-line engine with a power output of 99 kW and a dry weight of 134 kg. The engine was certified in 2006 and has since been used in combination with a 3-blade propeller manufactured by MT-Propeller Entwicklung. Aircraft powered by this engine are the Cessna 172 Skyhawk, the Piper PA 28 or the Robin DR400. (EASA 2015b, Technify Motors 2014)



Figure 2.3 DA40 NG (Diamond Aircraft 2023)

Another example is the 4-cylinder AE300 engine from Austro Engine. This company is a sister company of Diamond Aircraft. The engine delivers 123.5 kW and is also used in combination with a 3-blade variable pitch propeller from MT-Propeller Entwicklung. The engine is installed in several Diamond Aircraft models. One of them is the DA40 NG (Figure 2.3), which has a length of 8.06 m and a maximum take-off mass of 1310 kg and can carry a total of four passengers. (Austro Engine 2022, EASA 2015b, Diamond Aircraft 2023)

2.3.2 Otto Aviation Celera 500L

The Otto Aviation Celera 500L is a single-engine, six-passenger aircraft scheduled for delivery by 2025 (Figure 2.4). It is manufactured by the US company Otto Aviation Group. The shape of the fuselage is optimized for long laminar flow around the aircraft. Combined with a diesel engine from Germany's Raikhlin Aircraft Engine Developments, it is expected to offer the flexibility of a private jet with the comfort and cost of a commercial aircraft. The 12-cylinder piston engine can also run on Jet A1 fuel or kerosene and produces 368 kW, powering a five-blade propeller. The entire power train is optimized for high altitudes, as the aircraft is expected to operate at a mission altitude of 18 km. The power density is 1 kW/Kg and the power-specific fuel consumption (PSFC) is 210 g/kWh. (Otto Aviation 2021, RED Aircraft 2023, Quink 2022)



Figure 2.4 Otto Aviation Celera 500L (Steinke 2020)

3 Preliminary Sizing

The design of a diesel-powered aircraft is based on the Airbus A320-200, which is powered by two turbofan engines. Therefore, all major differences to the diesel configuration with piston engines have to be considered and implemented in the design. The first step is to develop a redesign of the A320-200, which will serve as the reference aircraft in the further stages of this project. This will be used to validate the top-level requirements and define specific values such as the payload mass. These values will be used to calculate all further designs to ensure a certain degree of comparability. A turboprop aircraft is then sized using the top-level requirements of the reference aircraft. This provides a more comparable aircraft than the reference aircraft due to its greater similarity to the piston engine with propeller. Finally, the turboprop aircraft is redesigned with a diesel engine. Due to the different power densities of the engines, this is done by taking a closer look at the operating empty mass ratio.

3.1 A320 with Turbofan (Reference Aircraft)

The Airbus A320 is a narrow-body aircraft used primarily on short- and medium-haul routes. The aircraft is a low-wing monoplane powered by two turbofan engines. The A320 200 is a version of the A320 that replaced the A320-100 and has a greater take-off mass and range. With a maximum take-off mass of 78000 kg, it can carry up to 180 passengers (Airbus 1985). The engines are either manufactured by International Aero Engines with the IAE V2500 engines or by CFM International with the CFM56 engines. While the CFM56 has been in service since 1988, the IAE-V2500 followed a year later (Frawley 2001). In this project, the CFM International engines are considered.

This work is based on the Airbus A320-200 in weight variant 017 (WV017). For this aircraft, the required masses and the wing area can be taken from Airbus 1985 (Table 3.1).

Table 3.1 Reference data Airbus A320-200 WV017 (Airbus 1985)

Name	Abbreviation	Value
Maximum Ramp Mass	m_{MR}	78400 kg
Maximum Take-Off Mass	m_{MTO}	78000 kg
Maximum Landing Mass	m_{ML}	66000 kg
Maximum Zero Fuel Mass	m_{MZF}	62500 kg
Operating Empty Mass	m_{OE}	42600 kg
Wing surface	S_W	122.60 m ²

The maximum take-off mass can be used to determine the runway length required for take-off (Figure 3.1). The airfield elevation is assumed to be at sea level. For a maximum take-off mass of 78000 kg (171961 lbs), the runway length is 2090 m (6857 ft).

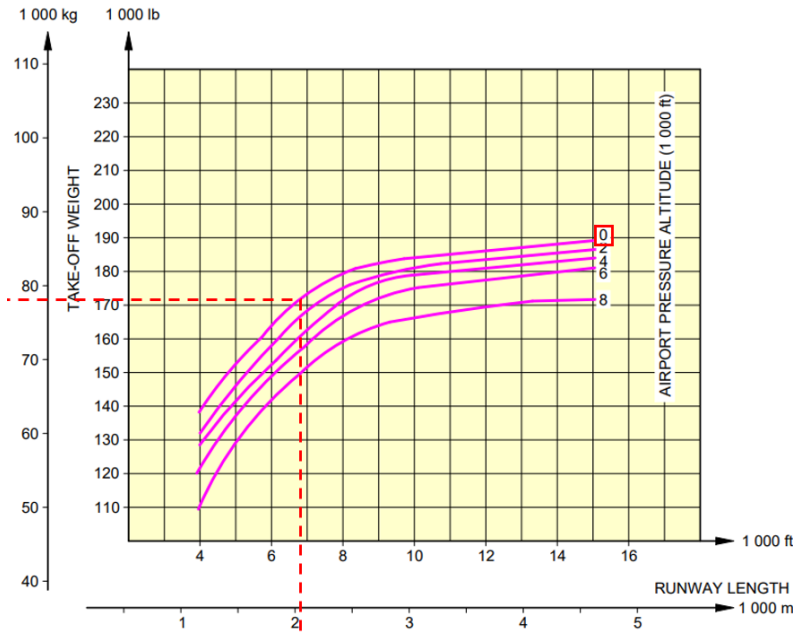


Figure 3.1 Runway length take-off (based on Airbus (1985))

The landing field length can be determined in the same way (Figure 3.2). For a maximum landing mass of 66000 kg (145505 lbs), the landing length is 1550 m (5085 ft).

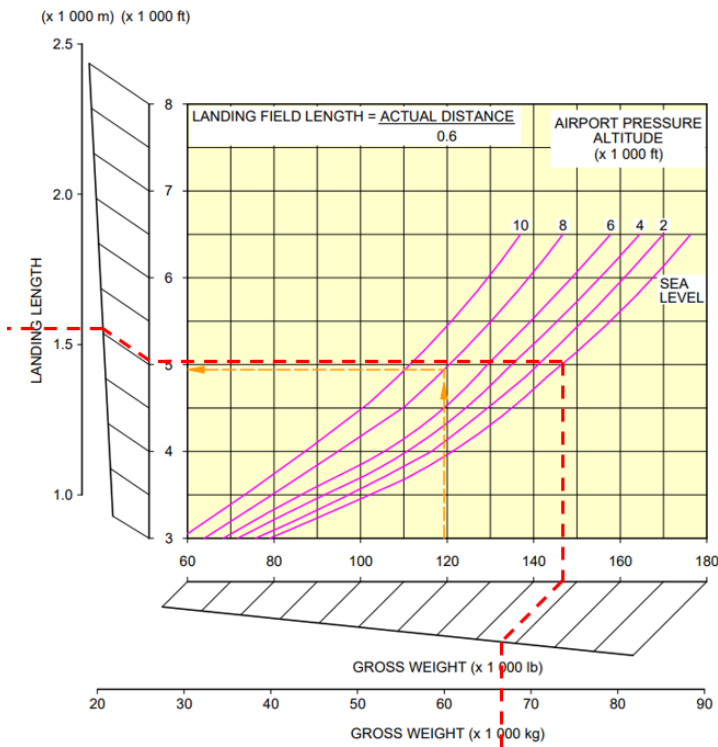


Figure 3.2 Landing field length (based on Airbus (1985))

The next step is to determine the range using the payload range diagram provided by Airbus 1985. Therefore, the point of maximum range at maximum payload is selected from Figure 3.3. With a maximum payload of 19700 kg, the range is 2125 NM. This corresponds to 3935.5 km and is almost equal to the distance between Abu Dhabi (United Arab Emirates) and Dhaka (Bangladesh), which is also flown by the A320. The cargo mass is not used for the moment, as it remains variable for the redesign. Further explanation follows in this chapter.

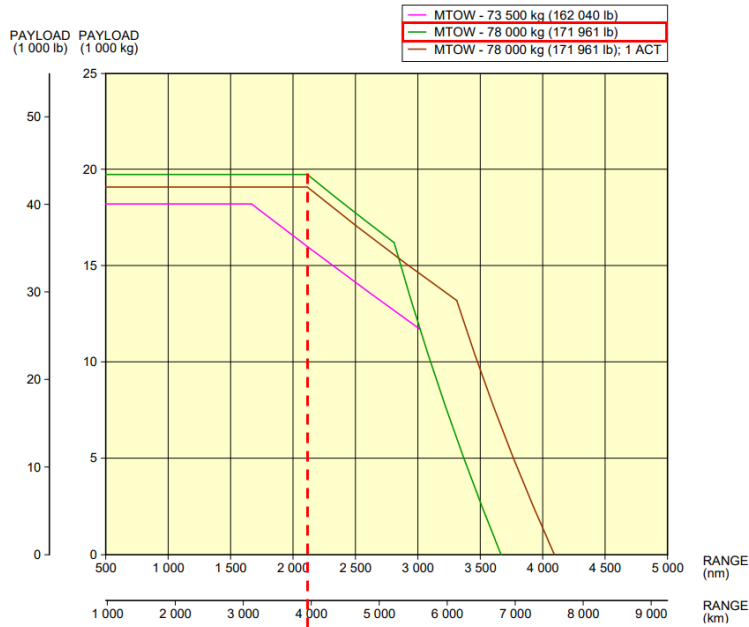


Figure 3.3 Payload-range diagram (based on Airbus (1985))

Besides the already mentioned top-level requirements, the Excel tool of Scholz (2023) requires many other input parameters. Most of them are standard or empirical values taken from Airbus (1985). Only a few values are considered in more detail. One of them is the aspect ratio. This can be calculated from the wing area and the span. The wing area is 122.6 m^2 and the span is 34.1 m (Airbus 1985, Modern Airlines 2023).

$$A_W = \frac{b_W^2}{S_W} = \frac{(34.1 \text{ m})^2}{122.6 \text{ m}^2} = 9.485 \quad (3.1)$$

The maximum glide ratio E_{max} can be taken from Raymer (2018). In the case of the A320-200, the glide ratio is 18.

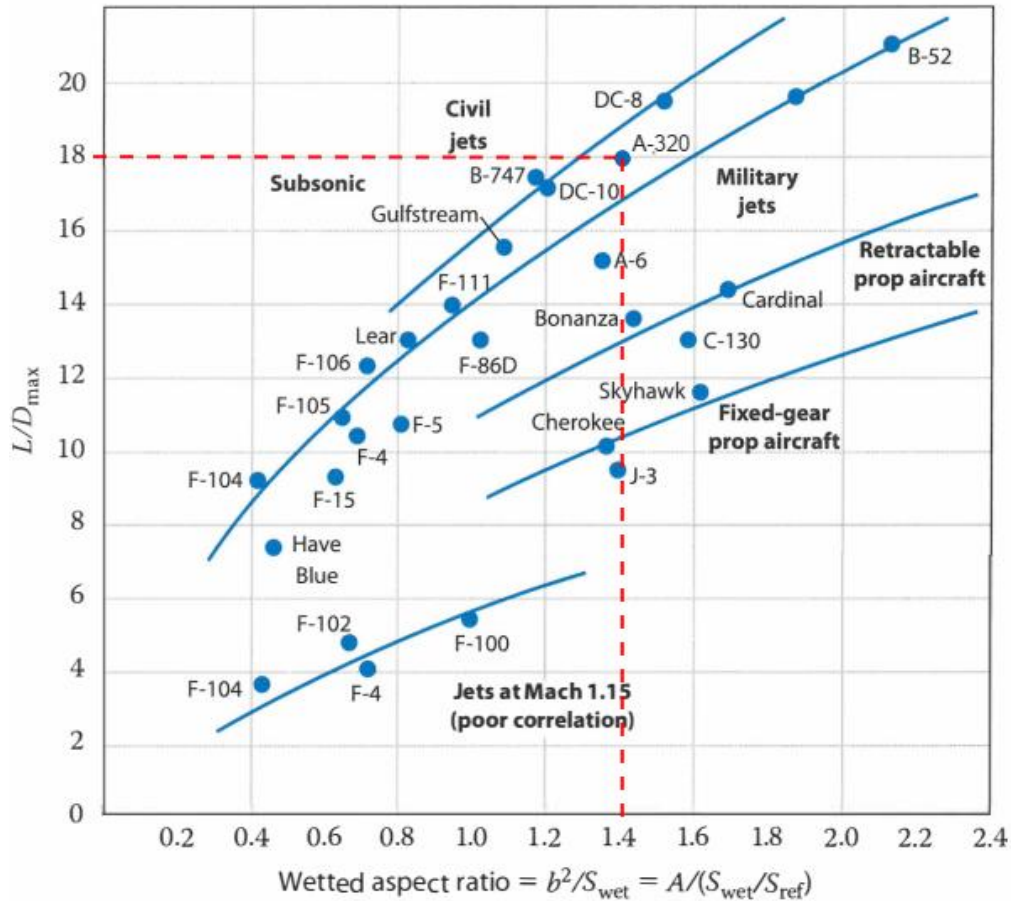


Figure 3.4 Maximum glide ratio (based on Raymer (2018))

The bypass ratio λ_{BPR} of the CFM56-5B4 is selected to be 5.7, while the thrust-specific fuel consumption c_{TSFC} is 15.4 mg/N/s (Meier 2021). The cruise speed is 0.78 Mach (Modern Airlines 2023).

The operating empty mass ratio is the ratio of the operating empty mass to the maximum take-off mass (m_{OE}/m_{MTO}) and has a significant influence on the total mass of the aircraft. The operating empty mass is the maximum take-off mass excluding fuel and payload. For the Airbus A320-200, this ratio is approximately 0.546 (Modern Airlines 2023).

All additional input parameters, as well as those just described, are summarized in Table A.1. Assuming an airfield at sea level, the density ratio σ is 1 and the take-off temperature corresponds to the ISA temperature (T_{ISA}) with 288.15 K. In addition, the American certification regulation FAR Part 25 applies, so the drag coefficient of the undercarriage is considered (Scholz 2020).

A value for V/V_{md} is now selected. This is done using the matching chart (Figure 3.5). The value is selected so that the line of the landing (vertical line) passes as closely as possible through the intersection of the cruise (bright blue) and take-off (yellow) graphs. The intersection point defines the thrust-to-weight ratio and the wing loading.

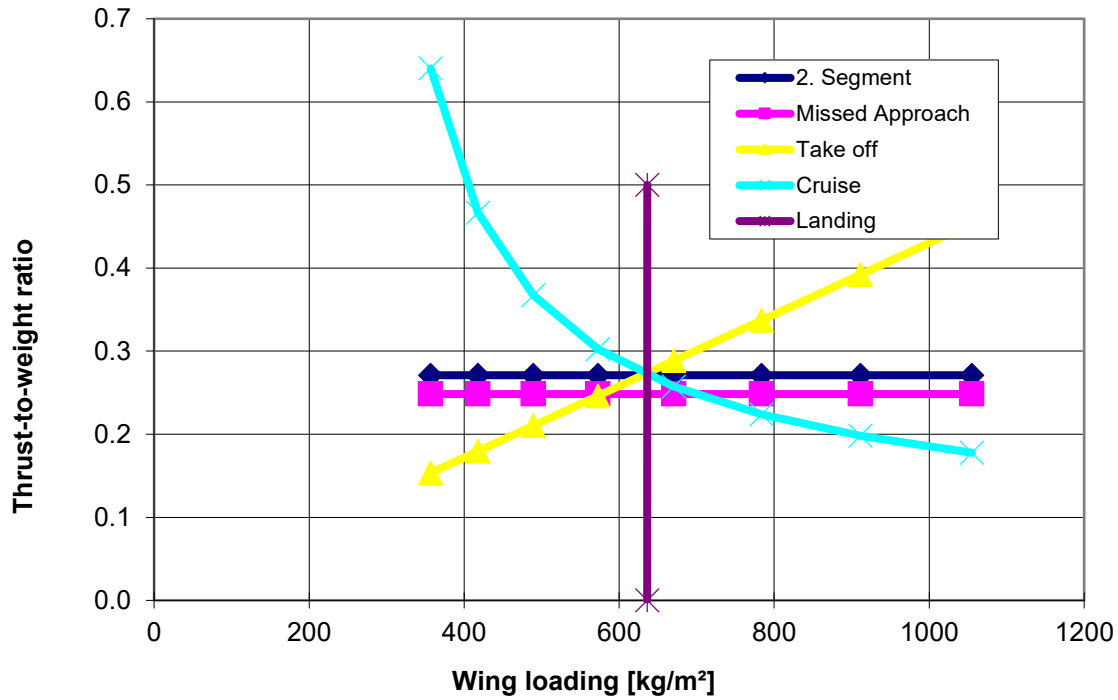


Figure 3.5 Matching Chart turboprop aircraft

According to Figure 3.5 the design is characterized by these three parameters:

- V/V_{md} : 1.015
- $T_{TO}/m_{MTO}/g$: 0.274
- m_{MTO}/S_w : 636 kg/m²

The final step is to define the payload. This consists of the mass of the passengers including their luggage and an additional cargo mass. For short- and medium-haul flights, a passenger mass of 93 kg is usually assumed (Scholz 2020). The number of passengers at maximum seating is 180, so the total passenger mass is known (Philippine Airlines 2023).

$$m_{PL} = n_{PAX} \cdot m_{PAX} + m_{cargo} \quad (3.2)$$

$$n_{PAX} \cdot m_{PAX} = 180 \cdot 93 \text{ kg} = 16740 \text{ kg} \quad (3.3)$$

The cargo mass is not specified in this project, but initially left variable. Then the value for the cargo mass is selected in the Excel tool at which the tool calculates a maximum take-off mass corresponding to the maximum take-off mass of the A320-200. This is the case for a cargo mass of 1230 kg. Using (3.2) the payload mass can now be determined.

$$m_{PL} = 16740 \text{ kg} + 1230 \text{ kg} = 17970 \text{ kg} \quad (3.4)$$

The payload mass of 17970 kg serves as a basis for the next aircraft designs. The Excel tool returns the values shown in Table 3.2 with the input parameters listed in Table A.1.

Table 3.2 Output data Excel tool turbofan aircraft

Parameter	Turbofan Redesign	A320-200
m_{MTO}	78000 kg	78000 kg
m_{ML}	66000 kg	66000 kg
m_{OE}	42600 kg	42600 kg
m_F	17430 kg	21195 kg
m_{PL}	17970 kg	19700
S_W	122.6 m ²	122.6 m ²
T_{TO}/n_E	104724 N	120102 N

The turbofan configuration was dimensioned to match the take-off mass of the reference aircraft. Due to the given mass ratios, the landing and operational empty mass as well as the wing area are identical to those of the A320-200 (Table 3.2). To achieve this, the payload mass was selected to match. The payload mass of the reference aircraft can be read from the payload range diagram (Figure 3.3) with a known range. The redesigned payload mass therefore differs by 1730 kg, which is a sufficient deviation in relation to the total mass of the aircraft.

The reference aircraft can carry up to 21195 kg of kerosene. This cannot be fully utilized at maximum payload due to the maximum take-off mass limitation (Modern Airlines 2023). In this case, 17430 kg of kerosene is required. The required thrust for each engine in the redesign is about 105 kN. The CFM56-5B4 used on the A320-200 can produce up to 120 kN of thrust per engine at a dry mass of 2381 kg (Meier 2021).

The top-level requirements selected in this chapter, as well as other input parameters, serve as the basis for the design of turboprop and diesel aircraft in the next chapters.

3.2 A320 with Turboprop

The next step is to size an airplane with turboprop engines. This is done using the Excel tool of Krull (2022), which can be found on Prof. Scholz's website.

The main input parameters are the top-level requirements validated in Chapter 3.1 and various parameters taken from the literature. The values for the parameters k_{APP} , k_L and k_{TO} are statistical values provided by Krull (2022). For the maximum lift coefficient ($C_{L,max,L}$), a value of 2.535 is chosen, since at this value the take-off wing loading m_{MTO}/S_W is equal to that of the reference aircraft.

The turboprop engine is based on the TP400-D6 engine data. This engine features a high power density of 4.15 kW/kg. Developed by the Europrop International consortium, this engine was specifically designed for the Airbus A400M military aircraft and delivers 8251 kW at a mass of approximately 1986.9 kg (depending on the direction of rotation). Its 8 blades result in a propeller area diameter of 5.5 m. The power-specific fuel consumption is 210 g/kWh (EASA 2021). The maximum glide ratio is set to the same value as the redesign for better comparability.

The cruise speed is reduced to 0.68 Mach because turboprop aircraft generally travel slower than turbofan aircraft (EASA 2015a).

In order to account for the engine power density that differs from that of turbofan aircraft, as well as to account for other mass differences, the operating empty mass ratio must be adjusted. First the statistical value of 0.535 is assumed and the turboprop aircraft is sized (Krull 2022). At a value of 0.91 for V/V_{md} , the matching chart provides a power-to-weight ratio of 283.9 W/kg and a wing loading of 636.2 kg/m² (Figure 3.6).

An overview of all input parameters is given in Table A.2. Now the operating empty mass ratio must be adjusted. This is done by breaking down the total aircraft mass of the turbofan aircraft into the individual system masses. These are determined as a percentage of the maximum take-off mass given by Braun (2020). However, the engine mass has to be corrected because the data is not up to date and today's engines have a higher power density. Using the required thrust calculated in Chapter 3.1 and the thrust-to-weight ratio of the reference engine CFM56-5B4 with 2.69 N/kg, the engine mass of the redesign can be determined (Meier 2021).

Since the operating empty mass of the Redesign is equal to the operating empty mass of the A320, which is known to be 0.546, the sum of all system masses that are part of the operating empty mass must be equal to this value (Modern Airlines 2023). To achieve this, the corresponding system masses are multiplied by a correction factor (Table 3.3).

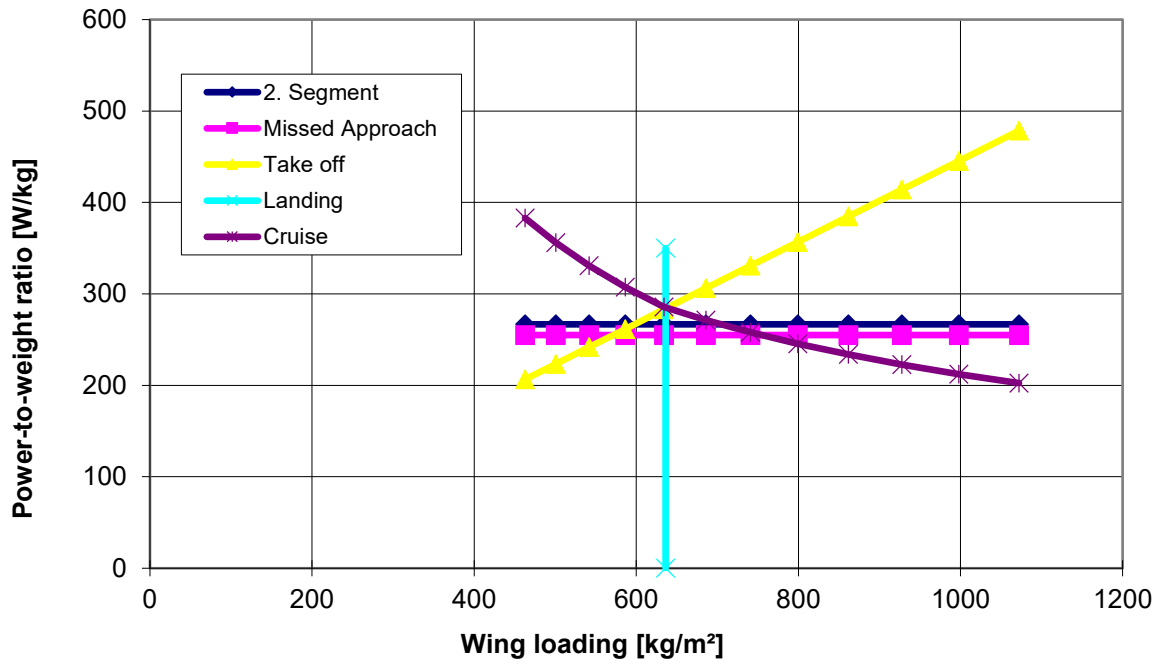


Figure 3.6 Matching Chart turboprop aircraft

Many of the system masses calculated for the turbofan design can be used for the turboprop design. For the sake of simplicity, the values in bold in the table are used for the conversion from turbofan to turboprop. For this purpose, all system masses to be changed are first specified as a function of the maximum take-off mass or the required total power. The required total power is given by the power-to-weight ratio as a function of the maximum take-off mass. In this way, all system masses depend only on the maximum take-off mass, which allows an iterative procedure to recalculate the maximum take-off mass and the new operating empty mass ratio.

$$P_{TO,TP} = \frac{P_{TO}}{m_{MTO}} \cdot m_{MTO,TP} \quad (3.5)$$

The new wing area is determined using the wing loading from the matching chart.

$$S_{W,TP} = \frac{1}{\frac{m_{MTO}}{S_W}} \cdot m_{MTO,TP} \quad (3.6)$$

Table 3.3 System masses turbofan aircraft

System	System masses [%]	System masses Turbofan [kg]	Corrected system masses Turbofan [kg]	System masses after correction [%]
Fuselage	11	8580	9054	11.61
Wing	13	10140	10700	13.72
H-Tail	1.1	858	905	1.16
V-Tail	0.7	546	576	0.74
Nacelle	0.8	624	658	0.84
Pylon	0.35	273	288	0.37
Undercarriage	5	3900	4115	5.28
Engine	5.05	3937	4154	5.33
Thrust rev.	0.8	624	658	0.84
Engine control	0.25	195	206	0.26
Fuel system	0.65	507	535	0.69
Oil system	0.35	273	288	0.37
APU	0.1	78	82	0.11
Flight con. sys.	1.5	1170	1235	1.58
Hydr. /pneu. Sys.	0.8	624	658	0.84
Electrical	1	780	823	1.06
Instrument	0.35	273	288	0.37
Avionics	0.25	195	206	0.26
ECS	0.7	546	576	0.74
Oxygen	0.25	195	206	0.26
Furnishing	5	3900	4115	5.28
Miscellaneous	0.25	195	206	0.26
Paint	0.01	8	8	0.01
Contingency	0.75	585	617	0.79
TOTAL		39005	41160	52.77
<i>m_{EW}/m_{MTO}</i>		0.5001	0.5277	
Crew	0.5	390	412	0.53
Consumable	1.25	975	1029	1.32
TOTAL	51.76	40370	42600	54.62
<i>m_{OE}/m_{MTO}</i>		0.5176	0.5462	
Payload		17970	17970	23.04
Fuel		17430	17430	22.35
TOTAL		75770	78000	100.00
TOTAL/m _{MTO}		0.9714	1.0000	

Using the mass per square meter of wing area of the turbofan aircraft, the new wing mass can be determined using the required wing area.

$$\frac{m_{W,TF}}{S_{W,TF}} = \frac{m_{W,TP}}{S_{W,TP}} = \text{const.} \quad (3.7)$$

$$m_{W,TP} = \frac{m_{W,TF}}{S_{W,TF}} \cdot S_{W,TP} \quad (3.8)$$

The horizontal and vertical tails are dimensioned as a function of the wing mass, since the size of the two tails depends on the wing area (Braun 2020). This is done by assuming that the ratio of wing mass to tail mass is constant. The wing masses can be replaced by (3.8), so that the mass of the tails depends only on the maximum take-off mass.

$$\frac{m_{H/V,TF}}{m_{W,TF}} = \frac{m_{H/V,TP}}{m_{W,TP}} = \text{const.} \quad (3.9)$$

$$m_{H/V,TP} = \frac{m_{W,TP}}{m_{W,TF}} \cdot m_{H/V,TF} \quad (3.10)$$

$$m_{H/V,TP} = \frac{\frac{m_{W,TF}}{S_{W,TF}} \cdot S_{W,TP}}{m_{W,TF}} \cdot m_{H/V,TF} \quad (3.11)$$

$$m_{H/V,TP} = \frac{S_{W,TP}}{S_{W,TF}} m_{H/V,TF} \quad (3.12)$$

The nacelle and pylon are sized according to the power required. Again, the mass to power ratio is assumed to be constant. Since the power has already been specified as a function of the maximum take-off mass in (3.5), the power can be replaced and the masses of the nacelle and pylon are only dependent on the maximum take-off mass.

$$\frac{m_{NA/PY,TF}}{P_{TO,TF}} = \frac{m_{NA/PY,TP}}{P_{TO,TP}} = \text{const.} \quad (3.13)$$

$$m_{NA/PY,TP} = \frac{P_{TO,TP}}{P_{TO,TF}} \cdot m_{NA/PY,TF} \quad (3.14)$$

$$m_{NA/PY,TP} = \frac{\frac{m_{MTO,TP}}{m_{MTO,TF}} \cdot P_{TO,TF}}{P_{TO,TF}} \cdot m_{NA/PY,TF} \quad (3.15)$$

$$m_{NA/PY,TP} = \frac{m_{MTO,TP}}{m_{MTO,TF}} \cdot m_{NA/PY,TF} \quad (3.16)$$

The undercarriage is dependent on the maximum take-off mass, where the ratio of undercarriage mass to maximum take-off mass is also assumed to be constant.

$$\frac{m_{UC,TF}}{m_{MTO,TF}} = \frac{m_{UC,TP}}{m_{MTO,TP}} = \text{const.} \quad (3.17)$$

$$m_{UC,TP} = \frac{m_{MTO,TP}}{m_{MTO,TF}} \cdot m_{UC,TF} \quad (3.18)$$

The engine mass depends on the total power required and the power density of the turboprop engine ($pd_{E,TP}$). The power density is 4.15 kW/kg (EASA 2021).

$$m_{E,TP} = P_{ges,TP} \cdot pd_{E,TP} \quad (3.19)$$

The required fuel mass can be determined from the fuel fraction of the total flight. The main difference is the power specific fuel consumption, which for the turboprop engine is 210 mg/W/h or $5.8 \cdot 10^{-8}$ kg/W/s. The cruise and loiter fuel fractions change by the Breguet factor. The mission fuel fraction m_F/m_{MTO} is approximately 0.227. Since the fuel fraction describes the ratio of consumed fuel mass to maximum take-off mass, it can be used to determine the required fuel mass.

$$m_F = 0.227 \cdot m_{MTO} \quad (3.20)$$

Since all variable masses now depend only on the maximum take-off mass, the maximum take-off mass can be determined by a target search in MS Excel. For this purpose, a maximum take-off mass is determined first, after which all individual system masses are calculated and summed. The sum results in a new maximum take-off mass, which is different from the first one. The target search determines the value at which the difference between the initial and final masses falls below a previously defined difference value. With the known system masses given in Table 3.4, the new value for the empty mass ratio of the aircraft can now be determined. In this case the empty mass ratio is 0.548. For verification purposes, this value is entered into the Excel sheet of Krull (2022) along with the other input parameters. The resulting maximum take-off mass is the same as that determined by the target search. The iteration results in a maximum take-off mass of 79584 kg. Table 3.5 shows further data given by the Excel sheet of Krull (2022).

Table 3.4 System masses turboprop aircraft

System	System masses Turbofan [kg]	System masses Turboprop [kg]	Difference (absolute) [kg]
Fuselage	9054	9054	0
Wing	10700	10917	217
H-Tail	905	924	18
V-Tail	576	588	12
Nacelle	658	672	13
Pylon	288	294	6
Undercarriage	4115	4199	84
Engine	4154	5442	1287
Thrust rev.	658	0	-658
Engine control	206	206	0
Fuel system	535	535	0
Oil system	288	288	0
APU	82	82	0
Flight con. sys.	1235	1235	0
Hydr. /pneu. Sys.	658	658	0
Electrical	823	823	0
Instrument	288	288	0
Avionics	206	206	0
ECS	576	576	0
Oxygen	206	206	0
Furnishing	4115	4115	0
Miscellaneous	206	206	0
Paint	8	8	0
Contingency	617	617	0
TOTAL	41160	42139	979
<i>m_{EW}/m_{MTO}</i>	0.5277	0.5295	0.0018
Crew	412	412	0
Consumable	1029	1029	0
TOTAL	42600	43579	979
<i>m_{OE}/m_{MTO}</i>	0.5462	0.5476	0.0014
Payload	17970	17970	0
Fuel	17430	18034	604
TOTAL	78000	79583	1583
TOTAL/m_{MTO}	100		

Table 3.5 Output data Excel tool turboprop aircraft

Parameter	Turboprop aircraft	Turbofan aircraft
m_{MTO}	79584 kg	78000 kg
m_{ML}	67340 kg	66000 kg
m_{OE}	43579 kg	42600 kg
m_F	18034 kg	17430 kg
m_{PL}	17970 kg	17970 kg
m_{OE}/m_{MTO}	0.548	0.546
S_W	125.1 m ²	122.6 m ²
$P_{TO}/n_E (T_{TO}/n_E)$	11298 kW	104724 N

A comparison shows that the masses of the turboprop aircraft are slightly higher than those of the turbofan aircraft. The difference in maximum take-off mass is 1584 kg, which is split between the operating empty mass and the required fuel mass. In the case of the operating empty mass, the difference is due to the almost 1300 kg heavier engine compared with the turbofan aircraft. However, the elimination of the thrust reverser can compensate for about half of the difference, since thrust reversal can be achieved by negative blade pitch. A detailed list of the individual system masses is given in Table 3.4. In addition to the increased operating empty mass, more fuel is required. This is due to the larger operating empty mass and the resulting larger maximum take-off mass, as well as a larger fuel fraction of the total flight.

At 11298 kW, the required power per engine is approximately 3000 kW higher than the 8251-kW benchmark engine. The TP400 is already the most powerful engine on the market. To solve this problem, either new engines can be designed or the total power required can be divided among four engines. However, dividing the power among four engines would require a new design. Due to the size of the engine, with a propeller disk diameter of 5.3 m, the turboprop aircraft is a high wing aircraft.

The problem here is the poor comparability between a jet engine and a turboprop engine. For one thing, the efficiency of the engine is still multiplied by the efficiency of the propeller, which is not the case with a jet engine (Mahfouz 2023). In addition, there are differences in this work due to the change in airspeed between turbofan and turboprop, which has an impact on wave drag (Scholz 2015). By further reducing the airspeed of the turboprop aircraft, fuel could be saved, which would also reduce the overall mass of the aircraft. This has already been done at Airport 2030, resulting in a reduction of the total mass (Johanning 2014). However, this would reduce the comparability of the different aircraft, which is why the airspeed was only slightly changed here to suit the turboprop aircraft.

In addition, the difference in cruise speed effects the flight duration. While the turbofan aircraft has a cruise speed of 0.78 Mach, the turboprop aircraft has a cruise speed of 0.68 Mach. At a range of about 2125 NM the additional flight time is about 35 minutes. This is the equivalent of flying from Abu Dhabi to Dhaka in about 4hrs 15min in a turbofan aircraft. The propeller aircraft therefore takes about 14% longer than the turbofan aircraft. This reduces the number of flights that can be made each day and therefore the profit that can be made.

3.3 A320 with Diesel Engine

The next step is to dimension an aircraft powered by diesel piston engines. The turboprop aircraft serves as the basis for this design, which is adapted by changing various parameters.

Not only does the specific fuel consumption change, but the lower power density of the piston engine must also be considered in the calculation. This can be achieved by adjusting the operating empty mass ratio. To achieve this, the influence of the engine mass on the aircraft empty mass ratio must be considered in more detail. In addition, the number of engines is increased.

Furthermore, the input parameters of the turboprop aircraft are used to ensure good comparability. As a result, the matching chart also provides the same values for the power-to-weight ratio and the wing loading at a ratio of 0.91 for V/V_{md} as for the turboprop aircraft (Figure 3.7). An overview of all input parameters can be found in Table A.3.

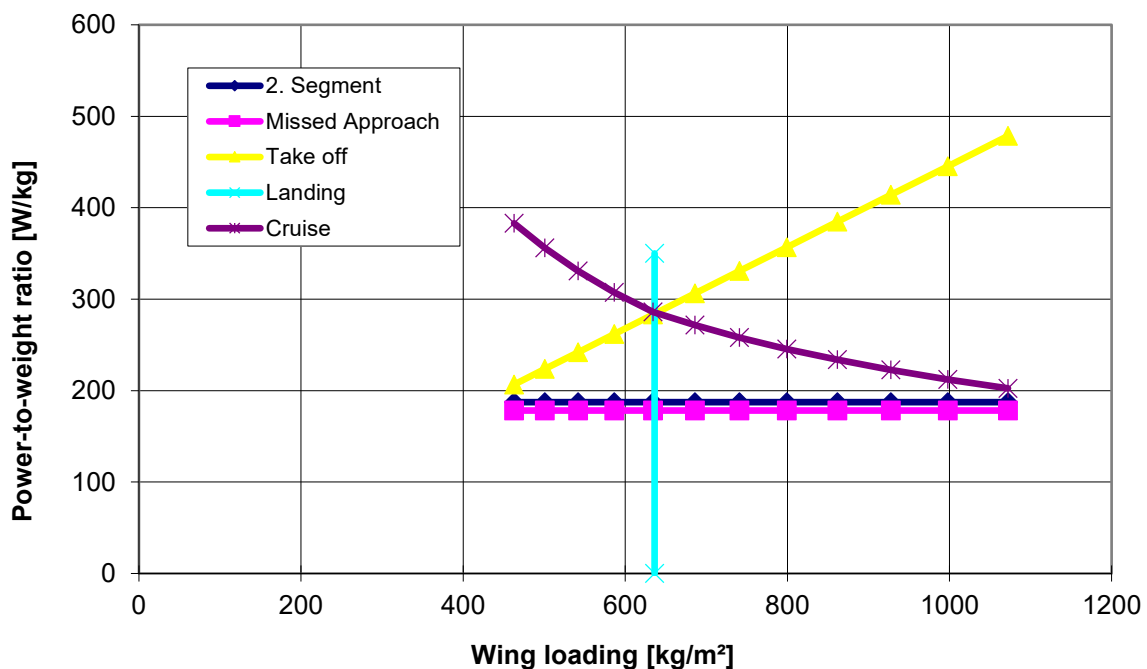


Figure 3.7 Matching Chart diesel aircraft

The operating empty mass ratio is set in the same way as in Chapter 3.2. However, the individual system masses do not have to be estimated as percentages, but can be taken from the final dimensioned turboprop aircraft (Table 3.4). The changing system masses are also the same as in Chapter 3.2 and are printed in bold in Table 3.6, with the exception of the thrust reversal, since this is also not considered separately in the turboprop aircraft.

Again, all the variable system masses are given as a function of the maximum take-off mass, which corresponds to the Equations (3.8) to (3.18), but with different indices.

The engine mass of the diesel engine depends on the total power required and the power density of the engine. The power density ($pd_{E,D}$) is assumed to be 1 kW/kg.

$$m_{E,D} = P_{ges,D} \cdot pd_{E,D} \quad (3.21)$$

The required fuel mass is determined by the fuel fraction. The power specific fuel consumption of the diesel engine is 210 mg/Wh or $5.8 \cdot 10^{-8}$ kg/W/s, similar to the turboprop engine. This results in an identical mission fuel fraction (3.22).

$$m_F/m_{MTO} = 0.227 \quad (3.22)$$

$$m_F = 0.227 \cdot m_{MTO} \quad (3.23)$$

Another major difference is the number of engines. Because of the expected higher maximum take-off mass due to the lower power density of the engines compared to the turboprop aircraft, the total power required is higher. Therefore, the power is now distributed over four engines instead of two.

The new system masses, the operating empty mass ratio and the new maximum take-off mass can now be determined using the target search in the Excel tool (Table 3.6).

When comparing the values calculated in Table 3.6 with those of the turboprop aircraft, the large difference in the maximum take-off mass is noticeable. This is mainly due to the increased operating empty mass, resulting from the low power density of the piston engines. Due to the close interaction of the individual aircraft systems, the masses of other systems also increase. Because of the increased total mass, the power must also be increased for a constant power-to-weight ratio, which again increases the engine mass and thus the total mass. To provide the additional power for the entire flight time, additional fuel is required. Ultimately, this results in an 80% increase in maximum take-off mass. Meanwhile, the fuel mass increases from 18034 kg to 32520 kg. Although the fuels are different, this has no significant effect on the fuel mass because the power specific fuel consumption of the two engines is the same.

Table 3.6 System masses diesel aircraft

System	System masses Turboprop [kg]	System masses Diesel [kg]	Difference absolute [kg]
Fuselage	9054	9054	0
Wing	10917	19686	8769
H-Tail	924	1666	742
V-Tail	588	1060	472
Nacelle	672	1211	540
Pylon	294	530	236
Undercarriage	4199	7572	3373
Engine	5442	40747	35305
Thrust rev.	0	0	0
Engine control	206	206	0
Fuel system	535	535	0
Oil system	288	288	0
APU	82	82	0
Flight con. sys.	1235	1235	0
Hydr. /pneu. Sys.	658	658	0
Electrical	823	823	0
Instrument	288	288	0
Avionics	206	206	0
ECS	576	576	0
Oxygen	206	206	0
Furnishing	4115	4115	0
Miscellaneous	206	206	0
Paint	8	8	0
Contingency	617	617	0
TOTAL	42139	91575	49437
<i>m_{EW}/m_{MTO}</i>	0.5295	0.6381	0.1086
Crew	412	412	0
Consumable	1029	1029	0
TOTAL	43579	93016	49437
<i>m_{OE}/m_{MTO}</i>	0.5476	0.6482	0.1006
Payload	17970	17970	0
Fuel	18034	32520	14485
TOTAL	79584	143506	63922
TOTAL/<i>m_{MTO}</i>	1.0000	1.0000	

Table 3.7 Mass comparison of all three engine types

Parameter	Turbofan aircraft	Turboprop aircraft	Rel. Diff. to TF A/C	Diesel aircraft	Rel. Diff. to TF A/C
m_{MTO}	78000 kg	79584 kg	2%	143506 kg	84%
m_{ML}	66000 kg	67340 kg	2%	121428 kg	84%
m_{OE}	42600 kg	43579 kg	2%	93016 kg	84%
m_F	17430 kg	18034 kg	3.5%	32520 kg	87%
m_{PL}	17970 kg	17970 kg	0%	17970 kg	0%
m_{OE}/m_{MTO}	0.546	0.548		0.648	
S_W	122.6 m ²	125.1 m ²	2%	225.6 m ²	84%
$P_{TO} (T_{TO})$	209448 N	22596 kW		40747 kW	
$P_{TO}/n_E (T_{TO}/n_E)$	104724 N	11298 kW		10187 kW	

Since the diesel aircraft has a high total power, the power must be distributed among four engines. Each engine provides 10187 kW of power (Table 3.7). Similar to the turboprop aircraft, the diesel aircraft can only be designed as a high wing aircraft due to the large propeller disc diameter.

Due to the significantly higher maximum take-off mass and therefore the higher fuel mass, it is clear that the diesel aircraft is neither ecologically nor economically viable. Therefore, a further calculation of the direct operating costs is unnecessary. The advantages of the piston engine, which are not only in the lower acquisition costs but also in the significantly lower maintenance intensity, cannot compensate for the additional costs of the extra fuel. The direct operating costs consist of many individual costs shown in (3.24).

$$C_{DOC} = C_{DEP} + C_{INT} + C_{INS} + C_F + C_M + C_C + C_{FEE} \quad (3.24)$$

The terms of the equation stand for:

- C_{DOC} : Direct operating costs
- C_{DEP} : Depreciation
- C_{INT} : Interest
- C_{INS} : Insurance
- C_F : Fuel
- C_M : Maintenance (airframe and power plant)
- C_C : Crew (cabin and cockpit)
- C_{FEE} : Fees and charges (landing, ATC, navigation or ground handling)

4 Preliminary Sizing for Shorter Range

In this chapter the range is reduced. The goal is to determine whether the heavy piston diesel aircraft can still be an alternative to the turboprop in the case of a lighter aircraft, given that half of all flights are short-haul (Statistisches Bundesamt 2021). The reduced range results in less fuel being required, which reduces the maximum take-off mass and the engines have to deliver less power. As a result, the low power density of the piston engines is less significant. The range is reduced from 2125 NM (LR) to 500 NM (SR). A turbofan aircraft will be sized first, before the other two engine types are considered.

4.1 A320 with Turbofan

The turbofan aircraft is dimensioned again with the tool of Scholz (2023). The input parameters can be found in Table B.1. However, some changes have to be made, because the required fuel mass decreases due to the reduced range and thus the maximum take-off mass. First, the operating empty mass ratio is adjusted. This is done in the same way as in Chapter 3.2 and Chapter 3.3 by splitting the maximum take-off mass among the individual system masses. As in Chapter 3.2, the new system masses are given as a function of the new maximum take-off mass ((3.8) to (3.18)) In contrast to the turboprop aircraft, the thrust reverser is not completely removed, but is reduced in size according to the new maximum take-off mass ((4.1)).

$$m_{TR,TF,SR} = \frac{m_{MTO,TF,SR}}{m_{MTO,TF,LR}} \cdot m_{TR,TF,LR} \quad (4.1)$$

Similarly, the new engine mass is now given as a function of the engine mass of the CFM56-5B4 turbofan engine installed on the A320-200.

$$m_{E,TF,SR} = \frac{m_{MTO,TF,SR}}{m_{MTO,TF,LR}} \cdot m_{CFM56-5B4} \quad (4.2)$$

In addition, the mass of the consumables is reduced due to the shorter range and resulting shorter flight time.

$$m_{CONS,SR} = 0.5 \cdot m_{CONS,LR} \quad (4.3)$$

All input parameters are shown in Table B.1. The resulting system masses, as well as the operating empty mass ratio and maximum take-off mass, are shown in Table 4.1 and Table 4.2.

Table 4.1 System masses turbofan aircraft (500 NM)

System	System masses Turbofan LR [kg]	System masses Turbofan SR [kg]	Difference (absolute) [kg]
Fuselage	9054	9054	0
Wing	10700	8856	-1844
H-Tail	905	749	-156
V-Tail	576	477	-99
Nacelle	658	545	-114
Pylon	288	238	-50
Undercarriage	4115	3406	-709
Engine	4154	3438	-716
Thrust rev.	658	545	-114
Engine control	206	206	0
Fuel system	535	535	0
Oil system	288	288	0
APU	82	82	0
Flight con. sys.	1235	1235	0
Hydr. /pneu. Sys.	658	658	0
Electrical	823	823	0
Instrument	288	288	0
Avionics	206	206	0
ECS	576	576	0
Oxygen	206	206	0
Furnishing	4115	4115	0
Miscellaneous	206	206	0
Paint	8	8	0
Contingency	617	617	0
TOTAL	41160	37358	-3802
<i>m_{EW}/m_{MTO}</i>	0.5277	0.5787	0.0510
Crew	412	412	0
Consumable	1029	514	-514
TOTAL	42600	38284	-4316
<i>m_{OE}/m_{MTO}</i>	0.5462	0.5930	0.0469
Payload	17970	17970	0
Fuel	17430	8301	-9129
TOTAL	78000	64555	-13445
TOTAL/ <i>m_{MTO}</i>	100	1.000	

In addition, the ratio of maximum landing mass to maximum take-off mass must be changed because less fuel is required due to the shorter flight distance ((4.4)). However, the ratio of wing area load during take-off does not change. The matching chart is shown in Figure 4.1.

$$\frac{m_{ML}}{m_{MTO}} = 0.932 \quad (4.4)$$

$$\frac{m_{MTO}}{S_W} = 636.15 \frac{\text{kg}}{\text{m}^2} \quad (4.5)$$

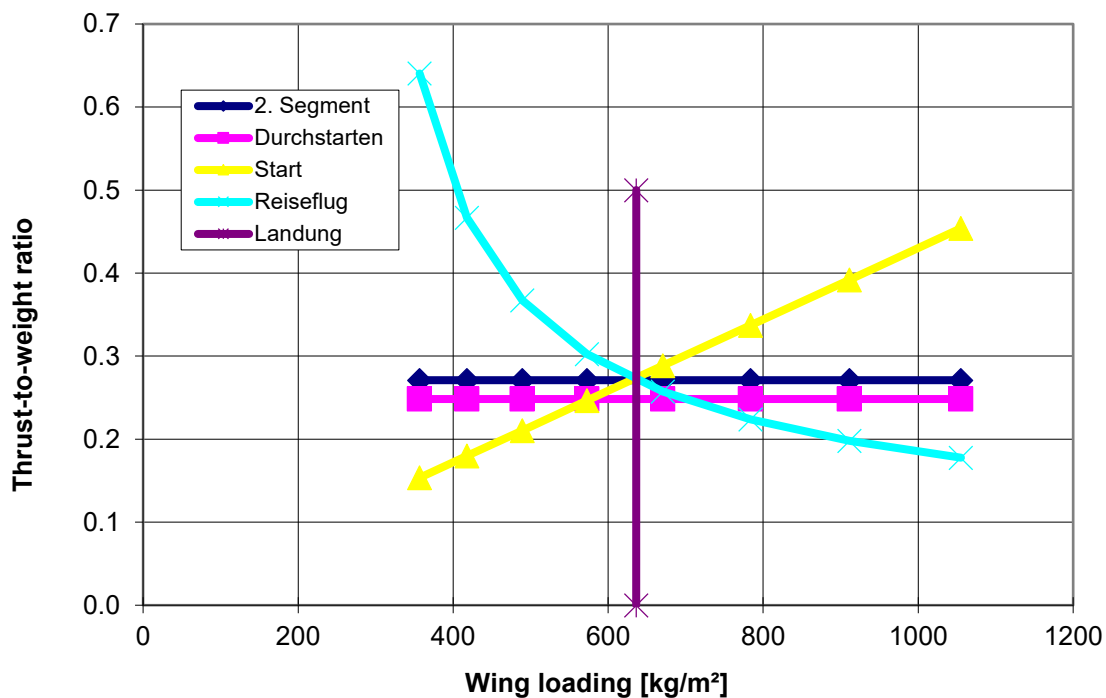


Figure 4.1 Matching Chart turboprop aircraft (500 NM)

Table 4.2 Output data Excel tool turboprop aircraft (500 NM)

Parameter	Turboprop aircraft SR	Turboprop aircraft LR
m_{MTO}	64555 kg	78000 kg
m_{ML}	60101 kg	66000 kg
m_{OE}	38284 kg	42600 kg
m_F	8301 kg	17430 kg
m_{PL}	17970 kg	17970 kg
m_{OE}/m_{MTO}	0.593	0.546
S_W	101.5 m ²	122.6 m ²
T_{TO}/n_E	86672 N	104724 N

This turbofan aircraft (SR) has a maximum take-off mass that is about 13.5 t less than that of the 2125 NM range aircraft (LR). The driving factor is the fuel mass, which is about 9 t less, which increases the operating empty mass ratio.

4.2 A320 with Turboprop

The turbofan aircraft is again dimensioned using the tool from Scholz (2023). The procedure is identical to Chapter 3.2. The new system masses can be taken from Table 4.3. The matching chart is shown in Figure 4.2. All input parameters are summarized in Table B.2.

The ratio of maximum landing mass to maximum take-off mass is the same as in Chapter 4.1.

$$\frac{m_{ML}}{m_{MTO}} = 0.932 \quad (4.6)$$

$$\frac{m_{MTO}}{S_W} = 636.15 \frac{\text{kg}}{\text{m}^2} \quad (4.7)$$

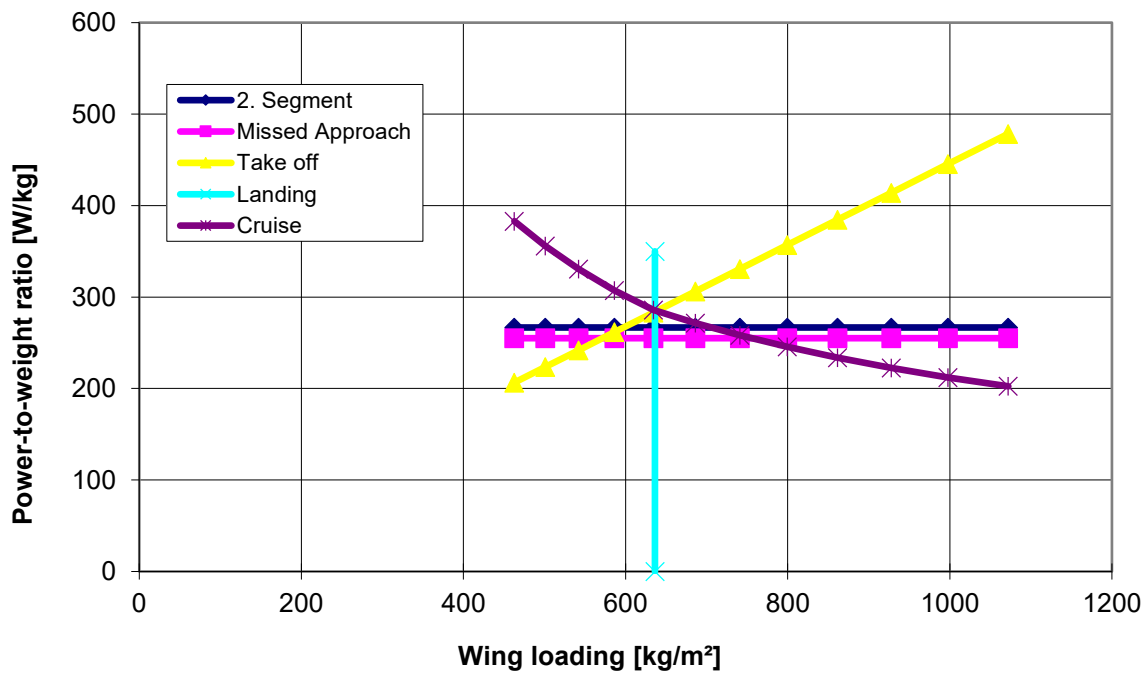


Figure 4.2 Matching Chart turboprop aircraft (500 NM)

Table 4.3 System masses turboprop aircraft (500 NM)

System	System masses Turbofan [kg]	System masses Turboprop [kg]	Difference (absolute) [kg]
Fuselage	9054	9054	0
Wing	8856	8944	88
H-Tail	749	757	7
V-Tail	477	482	5
Nacelle	545	550	5
Pylon	238	241	2
Undercarriage	3406	3440	34
Engine	3438	4458	1020
Thrust rev.	545	0	-545
Engine control	206	206	0
Fuel system	535	535	0
Oil system	288	288	0
APU	82	82	0
Flight con. sys.	1235	1235	0
Hydr. /pneu. Sys.	658	658	0
Electrical	823	823	0
Instrument	288	288	0
Avionics	206	206	0
ECS	576	576	0
Oxygen	206	206	0
Furnishing	4115	4115	0
Miscellaneous	206	206	0
Paint	8	8	0
Contingency	617	617	0
TOTAL	37358	37975	617
<i>m_{EW}/m_{MTO}</i>	0.5787	0.5824	0.0037
Crew	412	412	0
Consumable	514	514	0
TOTAL	38284	35411	-2872
<i>m_{OE}/m_{MTO}</i>	0.5930	0.5966	0.0036
Payload	17970	17970	0
Fuel	8301	8329	28
TOTAL	64555	65200	645
TOTAL/<i>m_{MTO}</i>	1.000	1.000	

Table 4.4 Output data Excel tool turboprop aircraft (500 NM)

Parameter	Turbofan aircraft	Turboprop aircraft
m_{MTO}	64555 kg	65200 kg
m_{ML}	60165 kg	60766 kg
m_{OE}	38284 kg	38901 kg
m_F	8301 kg	8329 kg
m_{PL}	17970 kg	17970 kg
m_{OE}/m_{MTO}	0.579	0.597
S_W	101.5 m ²	101.5 m ²
$T_{TO}/\eta_E (P_{TO}/\eta_E)$	86663 N	9255 kW

The maximum take-off mass of a turboprop aircraft is higher than that of the turbofan aircraft (Table 4.4). It also requires more fuel. Therefore, no difference in shorter range can be determined.

4.3 A320 with Diesel Engine

The diesel configuration is also calculated in the same way as in Chapter 3.3. The data of the turboprop aircraft with the shorter range are now used as reference values. The target search provides the following values for system mass, maximum take-off mass and required fuel mass (Table 4.5 and Table 4.6).

The ratio of maximum landing mass to maximum take-off mass is the same as in both chapters before.

$$\frac{m_{ML}}{m_{MTO}} = 0.932 \quad (4.8)$$

$$\frac{m_{MTO}}{S_W} = 636.15 \frac{\text{kg}}{\text{m}^2} \quad (4.9)$$

The matching chart is shown in Figure 4.3 and the summary of all input parameters is shown in Table B.3.

Table 4.5 System masses diesel aircraft (500 NM)

System	System masses Turboprop [kg]	System masses Diesel [kg]	Difference (absolute) [kg]
Fuselage	9054	9054	0
Wing	8944	14193	5249
H-Tail	757	1201	444
V-Tail	482	764	283
Nacelle	550	873	323
Pylon	241	382	141
Undercarriage	3440	5459	2019
Engine	4458	29375	24917
Thrust rev.	0	0	0
Engine control	206	206	0
Fuel system	535	535	0
Oil system	288	288	0
APU	82	82	0
Flight con. sys.	1235	1235	0
Hydr. /pneu. Sys.	658	658	0
Electrical	823	823	0
Instrument	288	288	0
Avionics	206	206	0
ECS	576	576	0
Oxygen	206	206	0
Furnishing	4115	4115	0
Miscellaneous	206	206	0
Paint	8	8	0
Contingency	617	617	0
TOTAL	34485	71351	36866
<i>m_{EW}/m_{MTO}</i>	0.5635	0.6896	0.1261
Crew	412	412	0
Consumable	514	514	0
TOTAL	35411	72277	36866
<i>m_{OE}/m_{MTO}</i>	0.5786	0.6986	0.1199
Payload	17970	17970	0
Fuel	7818	13217	5399
TOTAL	61199	103464	42265
TOTAL/m_{MTO}	1.0000	1.0000	

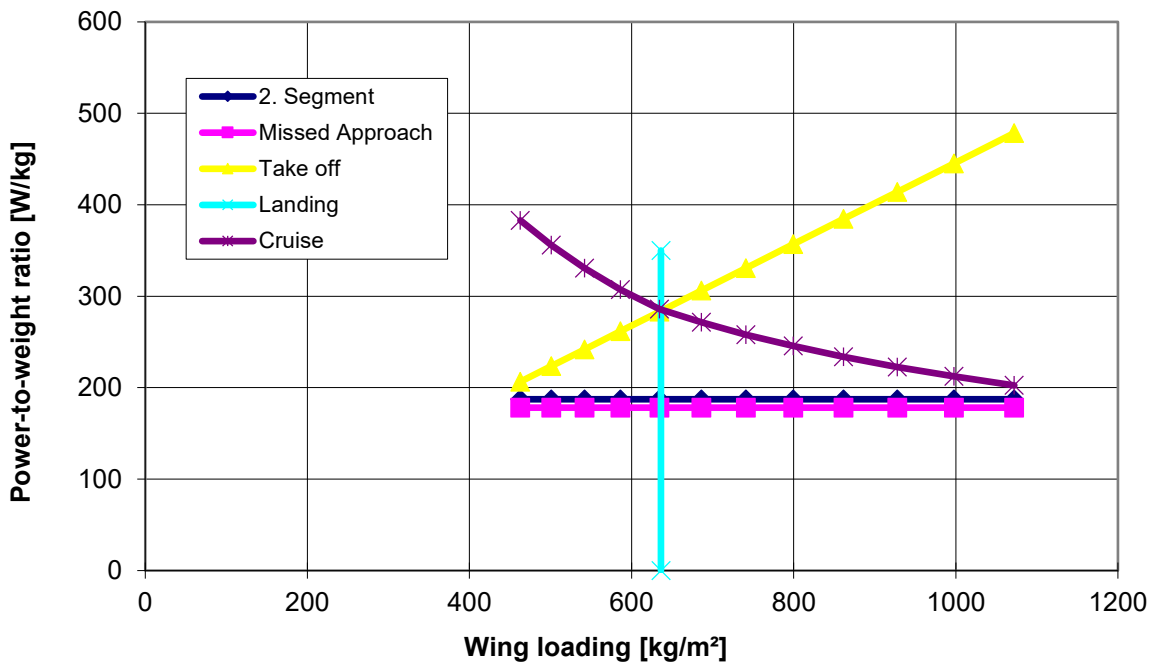


Figure 4.3 Matching Chart diesel aircraft (500 NM)

Table 4.6 Mass comparison of all three engine types (500 NM)

Parameter	Turbofan aircraft	Turboprop aircraft	Rel. Diff. to TF A/C	Diesel aircraft	Rel. Diff. to TF A/C
m_{MTO}	64555 kg	65200 kg	1%	103464 kg	60%
m_{ML}	54623 kg	60766 kg	1%	96429 kg	60%
m_{OE}	38284 kg	38901 kg	1%	72277 kg	60%
m_F	8301 kg	8329 kg	0.3%	13217 kg	59%
m_{PL}	17970 kg	17970 kg	0%	17970 kg	0%
m_{OE}/m_{MTO}	0.593	0.597		0.699	
S_w	101.5 m ²	101.5 m ²	0%	162.6 m ²	60%
$P_{TO} (T_{TO})$	173344 N	18511 kW		29375 kW	
$P_{TO}/n_E (T_{TO}/n_E)$	86672 N	9255 kW		7344 kW	

When comparing diesel and turboprop aircraft, it is clear that even with the shorter range, the diesel aircraft is significantly heavier. This is still due to the low power density of the diesel engines, which makes them 25 t heavier than the turboprop engines. Consequently, the operating empty mass ratio is also significantly higher. Because of the two additional engines, the power requirement per engine is lower, but the total power is greater than that of the turboprop. Since the diesel aircraft consumes 5 t more fuel than the turboprop aircraft, even with the shorter range, the diesel aircraft is neither ecologically nor economically viable.

5 Summary

The aim of the work was to investigate whether a diesel-powered A320 could be an alternative to the usual turbofan and turboprop aircraft. Especially in view of the global goal of reducing CO₂ emissions, the particularly efficient diesel engine came into play as a possible remedy and offered the possibility of undercutting the consumption of the classic jet engine. In addition, it remained unanswered in the literature why this had not been questioned earlier. The motivation for this work was to get to the bottom of this question.

First, various characteristics of past and present diesel engines were studied to provide a basis for preliminary sizing. Then, using the top-level requirements of the reference aircraft, the A320-200, three aircraft were designed. In addition to the diesel aircraft, these were a redesign of the A320 and a turboprop aircraft, which formed the basis for the diesel aircraft. The next step was to compare the three variants.

The A320-200 redesign with three different engines gave different results. The turbofan redesign was very close to the A320-200 benchmark, with only a small increase of the maximum take-off mass. The turboprop aircraft delivered slightly higher values in mass and wing area, but also consumed more fuel than the turbofan aircraft. However, the maximum take-off mass of the diesel aircraft is almost 65 t higher than that of the reference aircraft. This significantly increases the total power requirement of the diesel aircraft, which must be distributed over a total of four engines. Due to the dependence of fuel mass on power, the fuel requirement also increases significantly. This makes the use of diesel aircraft uneconomical. The higher mass of diesel aircraft is due to the lower power density of piston engines compared to turboprop and turbofan engines.

The next step was to reduce the range in order to look more closely at the dependency on maximum take-off mass. As a result, less fuel is required and the overall aircraft can be smaller due to the lower maximum take-off mass. To ensure that the same number of passengers and payload can be carried, the fuselage has not been modified. Although the diesel aircraft is now about 40 t lighter than the long-range version, it is still significantly heavier than the other two aircraft. As a result, its fuel mass is also higher, which still makes the diesel aircraft uneconomical.

The main problem in this work was the poor comparability of the turbofan aircraft with the turboprop aircraft due to the complete difference between the two engines. For example, the high efficiency of the diesel engine was still limited by the additional efficiency of the propeller, and the reduction in airspeed compared to the turbofan reduced the induced drag.

Nevertheless, it was important to make this comparison in order to gain a better understanding of the diesel engine's behavior and to answer some unanswered questions.

6 Conclusions and Recommendations

The comparison of the various aircraft with different engines has revealed clear differences. While turbofan and turboprop aircraft are very close in all masses, those of the diesel aircraft are significantly higher. The relatively low power density of piston engines has an enormous impact on the operating empty mass and thus also on the maximum take-off mass and the fuel mass. This disadvantage far outweighs all the advantages of diesel aircraft, which prevents them from being economically viable. Even reducing the range does not provide a sufficient improvement. In addition, the increase in flight time causes additional losses, which has a negative impact on direct operating costs, especially on longer routes.

In general, the values calculated in this paper should be treated with caution. They represent only a preliminary sizing of aircraft with different engines. They are based partly on data from the manufacturers of the reference aircraft, but also on data from other sources and on assumptions. The results are therefore only indicative and do not necessarily reflect reality. In addition, some systems were considered in a very simplified way, because the mass was assumed to be constant. In some cases, this is not the case in reality. For example, the size of the fuselage may be increased if additional fuel tanks are required due to the higher amount of fuel compared to the reference aircraft.

Another example is the diesel aircraft piston engine, which has a large influence on the design due to its low power density. The power density used comes from the RED A03-003 that can only deliver 368 kW (Chapter 2.1). If this is built on a much larger scale, no significant mass savings can be expected, but a slight improvement can still be expected. Increasing the number of cylinders may not result in an improvement, but there may be a mass saving if, for example, a larger pre-compressor is used for a larger number of cylinders. In addition, the aircraft piston engine technology has received much less attention than the turbofan engine over the past 30 years and has therefore not been developed to any great extent. As a result, there is still potential for optimizing this technology to improve power density.

The next step could be to change the top-level requirements. For example, by increasing the take-off distance, less power would be required, making the critical factor of low power density less relevant. This has already been done in the Airport 2030 project (Johanning 2014). The airspeed could also be further reduced.

List of References

- AIRBUS, 1985. *A320 – Aircraft Characteristics Airport and Maintenance Planning*. Blagnac Cedex, France: Airbus S.A.S.
 Available from: <https://bit.ly/493EMsM>
 Archived at: <https://perma.cc/WW52-4JJM>
- AUSTRO ENGINE, 2022. *E4 Series/AE300/AE330*. Wiener Neustadt, Austria: Austro Engine.
 Available from: <https://bit.ly/491g7Fj>
 Archived at: <https://perma.cc/TEZ6-FX86>
- BOYNE, Walter J., 2000. Air Force Aircraft of the Korean War. In: *Air Force Magazine*, vol. 83, no. 7, pp. 64-70.
 Available from: <https://bit.ly/3CI59eC>
 Archived at: <https://perma.cc/9QJX-E3H7>
- BOYNE, Walter J., 2006. The Rise and Fall of Donald Douglas. In: *Air Force Magazine*, vol. 89, no. 3, pp. 75-80.
 Available from: <https://bit.ly/3P0w1bs>
 Archived at: <https://perma.cc/J8AP-NEQD>
- BRAUN, Carsten, 2020. *Aircraft Design*. Lecture Notes. Aachen, Germany: Fachhochschule, Fachbereich Luft- und Raumfahrttechnik.
- CAMBRIDGE, 2023. *Modern*. Cambridge, United Kingdom: Cambridge University Press & Assessment.
 Available from: <https://dictionary.cambridge.org/dictionary/english/modern>
 Archived at: <https://perma.cc/S3ZX-ZPVR>
- CANTORE, Giuseppe, MATTARELLI, Enrico, RINALDINI, Carlo Alberto, 2014. A new design concept for 2-Stroke aircraft Diesel engines. In: *68th Conference of the Italian Thermal Machines Engineering Association, ATI2013*. Modena, Italy: Elsevier, vol. 45, pp. 739-748.
 Available from: <https://doi.org/10.1016/j.egypro.2014.01.079>
 Archived at: <https://perma.cc/5XP2-ALQB>

CARLUCCI, Antonio Paolo, FICARELLA, Antonio, LAFORGIA, Domenico, RENNA, Alessandro, 2015. Supercharging system behavior for high altitude operation of an aircraft 2-stroke Diesel engine. In: *Energy Conversion and Management*, vol. 101, pp. 470-480.

Available from: <https://doi.org/10.1016/j.enconman.2015.06.009>

Archived at: <https://perma.cc/H6D6-LPQ3>

CARLUCCI, Antonio Paolo, FICARELLA, Antonio, TRULLO, Gianluca, 2016. Performance optimization of a Two-Stroke supercharged diesel engine for aircraft propulsion. In: *Energy Conversion and Management*, vol. 122, pp. 279-289.

Available from: <https://doi.org/10.1016/j.enconman.2016.05.077>

Archived at: <https://perma.cc/UT9D-MR6F>

COLLINS, 2023a. *Passenger*. In: Collins Dictionaries.

Available from: <https://www.collinsdictionary.com/dictionary/english/passenger>

COLLINS, 2023b. *Aircraft*. In: Collins Dictionaries.

Available from: <https://www.collinsdictionary.com/dictionary/english/aircraft>

COLLINS, 2023c. *Diesel engine*. In: Collins Dictionaries.

Available from: <https://www.collinsdictionary.com/dictionary/english/diesel-engine>

COLLINS, 2023d. *Propeller*. In: Collins Dictionaries.

Available from: <https://www.collinsdictionary.com/dictionary/english/propeller>

DIAMOND AIRCRAFT, 2023. *DA40 Series*. Wiener Neustadt, Austria: Diamond Aircraft Industries.

Available from: <https://bit.ly/3MdCeOV>

Archived at: <https://perma.cc/8FVM-M3LX>

EASA, 2015a. *Type-Certificate Data Sheet EASA.A.169*: European Aviation Safety Agency.

Available from: <https://bit.ly/3CNUSb2>

Archived at: <https://perma.cc/J79T-B5KS>

EASA, 2015b. *Type-Certificate Data Sheet No. P.094*: European Aviation Safety Agency.

Available from: <https://bit.ly/3pcsfB8>

Archived at: <https://perma.cc/Q8NJ-YB9Z>

EASA, 2021. *Type-Certificate Data Sheet EASA.E.033*: European Aviation Safety Agency.

Available from: <https://bit.ly/3PwAjrf>

Archived at: <https://perma.cc/R6XS-Y9FJ>

EASA, 2023. *CS-25 Amendment 27*: European Aviation Safety Agency.

Available from: <https://bit.ly/448RraQ>

Archived at: <https://perma.cc/4H7J-ZZ8S>

FRAWLEY, Gerard, 2001. *The International Directory of Civil Aircraft*. Ramsbury, England: The Crowood Press Ltd. ISBN 978-1-84-037282-3.

GRABOWSKI, Łukasz, PIETRYKOWSKI, Konrad, KARPÍŃSKI, Paweł, 2017. Charging process analysis of an opposed-piston two-stroke aircraft Diesel engine. In: *ITM Web of Conferences*. Lublin, Poland, vol. 15, no. 03002, pp. 1-5.

Available from: <https://doi.org/10.1051/itmconf/20171503002>

Archived at: <https://perma.cc/X6U3-YC8J>

GRABOWSKI, Łukasz, PIETRYKOWSKI, Konrad, KARPÍŃSKI, Paweł, 2019. The zero-dimensional model of the scavenging process in the opposed-piston two-stroke aircraft diesel engine. In: *Propulsion and Power Research*, vol. 8, no. 4, pp. 300-309.

Available from: <https://doi.org/10.1016/j.jprr.2019.11.003>

Archived at: <https://perma.cc/5QG8-Y22Q>

HANSEN, Martin, 2021. Propeller. In: *Segelfliegen Grundausbildung*. Braunschweig: Deutscher Aeroclub.

Available from: <https://bit.ly/3CEH4Qa>

Archived at: <https://perma.cc/UPW5-CNMR>

JOHANNING, Andreas; SCHOLZ, Dieter, 2012. Novel Low-Flying Propeller-Driven Aircraft Concept for Reduced Direct Operating Costs and Emissions. In: *Proceedings : ICAS 2012 - 28th Congress of the International Council of the Aeronautical Sciences* (ICAS, Brisbane, 23.-28. September 2012). Edinburgh, UK: Optimage Ltd, 2012. - ISBN: 978-0-9565333-1-9.

Available from: https://www.icas.org/ICAS_ARCHIVE/ICAS2012/PAPERS/510.PDF

Archived at: <https://perma.cc/3JWB-ABJF>

JOHANNING, Andreas; SCHOLZ, Dieter, 2013. Smart Turboprop. In: *Ingenieurspiegel* (2013), no. 1, pp. 56-58, ISSN: 1868-5919.

Available from: <http://bit.ly/3FJujp8>

Archived at: <https://perma.cc/YBL4-7QYV>

JOHANNING, Andreas; SCHOLZ, Dieter, 2014. *Airport2030 – AP4.1: Configuration for Scenario 2015 (Possible A320 Successor)*. Airport2030, Final Presentation (Airbus, Hamburg, Germany, 2014-06-05).

Available from: <https://bit.ly/3FoaFii>

Archived at: <https://perma.cc/WG8H-ZEX7>

KRULL, Marlis, 2022. *Preliminary Sizing of Propeller Aircraft (Part 25)*. Project. Hamburg University of Applied Sciences, Aircraft Design and Systems Group (AERO).

Available from: <https://nbn-resolving.org/urn:nbn:de:gbv:18302-aero2022-04-29.012>

Archived at: <https://perma.cc/KA7E-PCVP>

LAGE, Helmuth, 2022. *Wie funktioniert ein Flugzeug-Propeller?*.

In: fliegermagazin, 2022-09-05.

Available from: <https://bit.ly/3qllHKX>

Archived at: <https://perma.cc/T85L-GYNK>

MAHFOUZ, Houssein, 2023. *Vergleich des Kraftstoffverbrauchs von Strahltriebwerken und Propellertriebwerken*. Project. Hamburg University of Applied Sciences, Aircraft Design and Systems Group (AERO).

Available from: <https://nbn-resolving.org/urn:nbn:de:gbv:18302-aero2023-02-02.013>

Archived at: <https://perma.cc/J8W7-G8WQ>

MEIER, Nathan, 2021. *Civil Turbojet/Turbofan Specifications*.

Available from: <https://www.jet-engine.net/civtfspec.htm>

Archived at: <https://perma.cc/AGF7-GX6B>

Mises, Richard, 1933. *Fluglehre*. Berlin: Springer.

ISBN 978-3-662-35891-7.

MODERN AIRLINERS, 2023. *Airbus A320*.

Available from: <https://www.modernairliners.com/airbus-a320>

Archived at: <https://perma.cc/TJ4J-GM7D>

MTU, 2023. *TP400-D6*. MTU Aero Engines AG.

Available from: <https://bit.ly/42P2R28>

Archived at: <https://perma.cc/8B53-XC2R>

NIȚĂ, Mihaela Florentina, 2008. *Aircraft Design Studies Based on the ATR 72*. Thesis. Hamburg University of Applied Sciences, Aircraft Design and Systems Group (AERO).

Available from: <https://www.fzt.haw-hamburg.de/pers/Scholz/arbeiten/TextNita.pdf>

Archived at: <https://perma.cc/SD77-YB6D>

NIȚĂ, Mihaela Florentina, 2013. *Contributions to Aircraft Preliminary Design and Optimization*. Dissertation. München: Verlag Dr. Hut, 2013.

Available from: <http://OPerA.ProfScholz.de>

Archived at: <https://perma.cc/U4CA-Z84M>

OTTO AVIATION, 2021. *Otto Aviation's Celera 500L Achieves a Total of 55 Successful Test Flights*. Yorba Linda, California, USA: Otto Aviation Group LLC.

Available from: <https://bit.ly/43VlgLx>

Archived at: <https://perma.cc/76JY-LVCL>

PHILIPPINE AIRLINES, 2023. *Airbus A320-200 (180-seater)*.

Available from: <https://bit.ly/3XlQUzW>

Archived at: <https://perma.cc/J9TM-X5QL>

QUINK, Sebastian, 2022. *Personal Communication*. Adenau, Germany.

RAYMER, Daniel P., 2018. *Aircraft Design: A Conceptual Approach, Sixth Edition*. Blacksburg, Virginia, USA: American Institute of Aeronautics and Astronautics, Inc.. ISBN 978-1-62410-490-9.

RED AIRCRAFT, 2023. *A03-003 and 005*. Adenau, Germany: Raikhlin Aircraft Engine Developments.

Available from: <https://Red-Aircraft.de/red-a03-003>

Archived at: <https://perma.cc/65HG-86BW>

SÀNCHEZ BARREDA, Victor Julián, 2013. *Conceptual Design Optimization of a Strut Braced Wing Aircraft*. Master Thesis, Hamburg University of Applied Sciences.

Available from: <https://www.fzt.haw-hamburg.de/pers/Scholz/arbeiten/TextSanchez.pdf>

Archived at: <https://perma.cc/T6SR-D3AS>

SCHOLZ, Dieter; NIȚĂ, Mihaela Florentina, 2009. Preliminary Sizing of Large Propeller Driven Aeroplanes. In: *Czech Aerospace Proceedings*, vol. 2009, no. 2, pp. 41-47, ISSN: 1211-877X.

Available from: <https://bit.ly/46YyWqV>

Archived at: <https://perma.cc/GCM3-4RZ3>

SCHOLZ, Dieter; JOHANNING, Andreas, 2014. *Smart Turboprop – A Possible A320 Successor*. Presentation (4th Symposium on Collaboration in Aircraft Design, Toulouse, France, 2014-11-25 to 2014-11-27).

Available from: <https://bit.ly/3SjFXhS>

Archived at: <https://perma.cc/6MTZ-MA5V>

SCHOLZ, Dieter, 2015. *Aircraft Design*. Lecture Notes. Hamburg University of Applied Sciences.

Available from: <http://LectureNotes.AircraftDesign.org>

- SCHOLZ, Dieter, 2020. *Berechnungsschema zur Flugzeug-Dimensionierung für Strahlverkehrsflugzeug und Business Jets Zulassungsbasis: JAR-25 bzw. FAR Part 25*. Lecture Notes. Hamburg University of Applied Sciences.
Available from: <https://bit.ly/3M5feSa>
Archived at: <https://perma.cc/3PRX-X4R3>
- SCHOLZ, Dieter, 2023. *PreSTo - Aircraft Preliminary Sizing Tool*. Excel Table. Hamburg University of Applied Sciences, Aircraft Design and Systems Group (AERO).
Available from: <http://PreSTo.ProfScholz.de>
Archived at: <https://perma.cc/VB5E-JJKT>
- STATISTISCHES BUNDESAMT, 2021. *Mehr als die Hälfte aller Passagierflüge in Deutschland waren 2020 Kurzstreckenflüge*.
Available from: <https://bit.ly/46uWvb5>
Archived at: <https://perma.cc/TQ6P-YJWM>
- STEINHAUSEN, Markus, SCHOLZ, Dieter, 2022. *Fliegen mit Dieselmotor und Propeller – spart Kraftstoff und hilft der Umwelt*.
Available from: <https://purl.org/aero/PR2022-01-28>
Archived at: <https://perma.cc/E2BU-M5UE>
- STEINKE, Sebastian, 2020. Sparflugzeug Celera 500L in der Flugerprobung. In: *Flug Revue*, 2020-08-27.
Available from: <https://bit.ly/42ORBTH>
Archived at: <https://perma.cc/DXS2-YA76>
- TECHNIFY MOTORS, 2014. *Flugmotor Aircraft Engine CD-135*. St. Egidien, Germany: Technify Motors.
Available from: <http://continentaldiesel.com/typo3/index.php?id=59>
Archived at: <https://perma.cc/2WEV-E7ZL>
- XU, Zheng, JI, Fenzhu, DING, Shuiting, ZHAO, Yunhai, ZHOU, Yu, ZHANG, Qi, DU, Farong, 2021. Effect of scavenge port angles on flow distribution and performance of swirl-loop scavenging in 2-stroke aircraft diesel engine. In: *Chinese Journal of Aeronautics*, vol. 34, no. 3, pp. 105-117.
Available from: <https://doi.org/10.1016/j.cja.2020.07.015>
Archived at: <https://perma.cc/NBA4-ACZH>

All online resources have been accessed on 2023-10-07 or later.

Appendix A – Input Parameter Long Range

Table A.1 Input data Excel tool turbofan aircraft

Segment/ Category	Parameter	Abbreviation	Value
Approach/ Landing	Approach factor	k_{APP}	1.7
	Safety landing distance	SL_{FL}	1550 m
	Mass ratio landing/take-off	m_{ML}/m_{MTO}	0.846
	Wing loading at landing mass	m_{ML}/S_W	538.34 kg/m ²
Take-off	Safety start distance	S_{TOFL}	2090 m
	Start temperature above ISA (288.15K)	ΔT_{TO}	0 K
	Density ratio	σ	1
	Take-off factor	k_{TO}	2.34
2nd Segment	Aspect ratio	A	9.485
	Zero drag coefficient (clean)	$C_{D,0}$	0.02
	Zero drag coefficient (slats)	$\Delta C_{D,slat}$	0
	Oswald factor; with flap deflection	e	0.75
	Number of engines	n_E	2
Missed Approach	Zero drag coefficient (clean)	$C_{D,0}$	0.02
	Zero drag coefficient (slats)	$\Delta C_{D,slat}$	0
	Zero drag coefficient (undercarriage)	$\Delta C_{D,UC}$	0.015
Cruise	Max. glide ratio	E_{max}	18
	Bypass ratio	λ_{BPR}	5.7
	Oswald factor (clean)	e	0.85
	Mach number (Cruise)	M_{CR}	0.78
		V/V_{md}	1.015
	Design range	R	2125 NM
	Flight distance to alternate airport	$S_{TO,alternate}$	200 NM
	FAR Part 21-Reserves: international Specific fuel consumption	C_{CR}	$1.5 \cdot 10^{-5}$ kg/N/s
Fuel Fraction	Fuel-Fraction (engine start)	$M_{ff,E}$	0.990
	Fuel-Fraction (Taxi)	$M_{ff,T}$	0.995
	Fuel-Fraction, (Take-Off)	$M_{ff,TO}$	0.995
	Fuel-Fraction (Climb)	$M_{ff,CLB}$	0.980
	Fuel-Fraction (Descent)	$M_{ff,DES}$	0.990
	Fuel-Fraction (Landing)	$M_{ff,L}$	0.992
General	Operating empty mass ratio	m_{OE}/m_{MTO}	0.546
	Passenger mass with luggage (short/ medium haul)	m_{PAX}	93 kg
	Number of passengers	n_{PAX}	180
	Cargo mass	m_{cargo}	1230 kg

Table A.2 Input data Excel tool turboprop aircraft

Segment/ Category	Parameter	Abbreviation	Value
Approach/ Landing	Approach factor	k_{APP}	1.939
	Safety landing distance	S_{LFL}	1550 m
	Mass ratio landing/take-off	m_{ML}/m_{MTO}	0.846
	Wing loading at landing mass	m_{ML}/S_W	538.34 kg/m ²
Take-off	Safety start distance	S_{TOFL}	2090 m
	Start temperature above ISA (288.15K)	ΔT_{TO}	0 K
	Density ratio	σ	1
	Take-off factor	k_{TO}	2.25
	Propeller disc diameter	d_{disc}	5.30 m
	Take-off power of one engine (reference)	$P_{S,TO}/n_E$	8251000 W
	Propeller efficiency	η_P	0.65
2nd Segment	Aspect ratio	A	9.485
	Zero drag coefficient (clean)	$C_{D,0}$	0.02
	Zero drag coefficient (slats)	$\Delta C_{D,slat}$	0
	Oswald factor; with flap deflection	e	0.75
	Number of engines	n_E	2
	Propeller efficiency	η_P	0.65
Missed Approach	Zero drag coefficient (clean)	$C_{D,0}$	0.02
	Zero drag coefficient (slats)	$\Delta C_{D,slat}$	0
	Zero drag coefficient (undercarriage)	$\Delta C_{D,UC}$	0.015
	Propeller efficiency	η_P	0.64
Cruise	Max. glide ratio	E_{max}	18
	Oswald factor (clean)	e	0.85
	Mach number (Cruise)	M_{CR}	0.68
	Propeller efficiency	η_P	0.85
		V/V_{md}	0.910
	Design range	R	2125 NM
	Flight distance to alternate airport FAR Part 21-Reserves: international	$S_{TO,alternate}$	200 NM
	Specific fuel consumption	C_{CR}	$5.8 \cdot 10^{-8}$ kg/W/s
Fuel Fraction	Fuel-Fraction (engine start)	$M_{ff,E}$	0.990
	Fuel-Fraction (Taxi)	$M_{ff,T}$	0.995
	Fuel-Fraction, (Take-Off)	$M_{ff,TO}$	0.995
	Fuel-Fraction (Climb)	$M_{ff,CLB}$	0.985
	Fuel-Fraction (Descent)	$M_{ff,DES}$	0.985
	Fuel-Fraction (Landing)	$M_{ff,L}$	0.995
General	Operating empty mass ratio	m_{OE}/m_{MTO}	0.546
	Passenger mass with luggage (short/ medium haul)	m_{PAX}	93 kg
	Number of passengers	n_{PAX}	180
	Cargo mass	m_{cargo}	1230 kg

Table A.3 Input data Excel tool diesel aircraft

Segment/ Category	Parameter	Abbreviation	Value
Approach/ Landing	Approach factor	K_{APP}	1.939
	Safety landing distance	S_{LFL}	1550 m
	Mass ratio landing/take-off	m_{ML}/m_{MTO}	0.846
	Wing loading at landing mass	m_{ML}/S_W	538.34 kg/m ²
Take-off	Safety start distance	S_{TOFL}	2090 m
	Start temperature above ISA (288.15K)	ΔT_{TO}	0 K
	Density ratio	σ	1
	Take-off factor	k_{TO}	2.25
	Propeller disc diameter	d_{disc}	5.30 m
	Take-off power of one engine (reference)	$P_{S,TO}/n_E$	8251000 W
	Propeller efficiency	η_P	0.65
2nd Segment	Aspect ratio	A	9.485
	Zero drag coefficient (clean)	$C_{D,0}$	0.02
	Zero drag coefficient (slats)	$\Delta C_{D,slat}$	0
	Oswald factor; with flap deflection	e	0.75
	Number of engines	n_E	4
	Propeller efficiency	η_P	0.65
Missed Approach	Zero drag coefficient (clean)	$C_{D,0}$	0.02
	Zero drag coefficient (slats)	$\Delta C_{D,slat}$	0
	Zero drag coefficient (undercarriage)	$\Delta C_{D,UC}$	0.015
	Propeller efficiency	η_P	0.64
Cruise	Max. glide ratio	E_{max}	18
	Oswald factor (clean)	e	0.85
	Mach number (Cruise)	M_{CR}	0.68
	Propeller efficiency	η_P	0.85
		V/V_{md}	0.910
	Design range	R	2125 NM
	Flight distance to alternate airport FAR Part 21-Reserves: international	$S_{TO,alternate}$	200 NM
	Specific fuel consumption	C_{CR}	$5.8 \cdot 10^{-8}$ kg/W/s
Fuel Fraction	Fuel-Fraction (engine start)	$M_{ff,E}$	0.990
	Fuel-Fraction (Taxi)	$M_{ff,T}$	0.995
	Fuel-Fraction, (Take-Off)	$M_{ff,TO}$	0.995
	Fuel-Fraction (Climb)	$M_{ff,CLB}$	0.985
	Fuel-Fraction (Descent)	$M_{ff,DES}$	0.985
	Fuel-Fraction (Landing)	$M_{ff,L}$	0.995
General	Operating empty mass ratio	m_{OE}/m_{MTO}	0.644
	Passenger mass with luggage (short/ medium haul)	m_{PAX}	93 kg
	Number of passengers	n_{PAX}	180
	Cargo mass	m_{cargo}	1230 kg

Appendix B - Input Parameter Short Range

Table B.1 Input data Excel tool turbofan aircraft (500 NM)

Segment/ Category	Parameter	Abbreviation	Value
Approach/ Landing	Approach factor	K_{APP}	1.7
	Safety landing distance	S_{LFL}	1550 m
	Mass ratio landing/take-off	m_{ML}/m_{MTO}	0.932
	Wing loading at take-off mass	m_{ML}/S_W	636.15 kg/m ²
Take-off	Safety start distance	S_{TOFL}	2090 m
	Start temperature above ISA (288.15K)	ΔT_{TO}	0 K
	Density ratio	σ	1
	Take-off factor	k_{TO}	2.34
2nd Segment	Aspect ratio	A	9.485
	Zero drag coefficient (clean)	$C_{D,0}$	0.02
	Zero drag coefficient (slats)	$\Delta C_{D,slat}$	0
	Oswald factor; with flap deflection	e	0.75
	Number of engines	n_E	2
Missed Approach	Zero drag coefficient (clean)	$C_{D,0}$	0.02
	Zero drag coefficient (slats)	$\Delta C_{D,slat}$	0
	Zero drag coefficient (undercarriage)	$\Delta C_{D,UC}$	0.015
Cruise	Max. glide ratio	E_{max}	18
	Bypass ratio	λ_{BPR}	5.7
	Oswald factor (clean)	e	0.85
	Mach number (Cruise)	M_{CR}	0.78
		V/V_{md}	1.015
	Design range	R	500 NM
	Flight distance to alternate airport	$S_{TO,alternate}$	200 NM
	FAR Part 21-Reserves: international Specific fuel consumption	C_{CR}	$1.5 \cdot 10^{-5}$ kg/N/s
Fuel Fraction	Fuel-Fraction (engine start)	$M_{ff,E}$	0.990
	Fuel-Fraction (Taxi)	$M_{ff,T}$	0.995
	Fuel-Fraction, (Take-Off)	$M_{ff,TO}$	0.995
	Fuel-Fraction (Climb)	$M_{ff,CLB}$	0.980
	Fuel-Fraction (Descent)	$M_{ff,DES}$	0.990
	Fuel-Fraction (Landing)	$M_{ff,L}$	0.992
General	Operating empty mass ratio	m_{OE}/m_{MTO}	0.593
	Passenger mass with luggage (short/ medium haul)	m_{PAX}	93 kg
	Number of passengers	n_{PAX}	180
	Cargo mass	m_{cargo}	1230 kg

Table B.2 Input data Excel tool turboprop aircraft (500 NM)

Segment/ Category	Parameter	Abbreviation	Value
Approach/ Landing	Approach factor	k_{APP}	1.939
	Safety landing distance	S_{LFL}	1550 m
	Mass ratio landing/take-off	m_{ML}/m_{MTO}	0.932
	Wing loading at take-off mass	m_{ML}/S_W	636.15 kg/m ²
Take-off	Safety start distance	S_{TOFL}	2090 m
	Start temperature above ISA (288.15K)	ΔT_{TO}	0 K
	Density ratio	σ	1
	Take-off factor	k_{TO}	2.25
	Propeller disc diameter	d_{disc}	5.30 m
	Take-off power of one engine (reference)	$P_{S,TO}/n_E$	8251000 W
	Propeller efficiency	η_P	0.65
2nd Segment	Aspect ratio	A	9.485
	Zero drag coefficient (clean)	$C_{D,0}$	0.02
	Zero drag coefficient (slats)	$\Delta C_{D,slat}$	0
	Oswald factor; with flap deflection	e	0.75
	Number of engines	n_E	2
	Propeller efficiency	η_P	0.65
Missed Approach	Zero drag coefficient (clean)	$C_{D,0}$	0.02
	Zero drag coefficient (slats)	$\Delta C_{D,slat}$	0
	Zero drag coefficient (undercarriage)	$\Delta C_{D,UC}$	0.015
	Propeller efficiency	η_P	0.64
Cruise	Max. glide ratio	E_{max}	18
	Oswald factor (clean)	e	0.85
	Mach number (Cruise)	M_{CR}	0.68
	Propeller efficiency	η_P	0.85
		V/V_{md}	0.910
	Design range	R	500 NM
	Flight distance to alternate airport FAR Part 21-Reserves: international	$S_{TO,alternate}$	200 NM
	Specific fuel consumption	C_{CR}	$5.8 \cdot 10^{-8}$ kg/W/s
Fuel Fraction	Fuel-Fraction (engine start)	$M_{ff,E}$	0.990
	Fuel-Fraction (Taxi)	$M_{ff,T}$	0.995
	Fuel-Fraction, (Take-Off)	$M_{ff,TO}$	0.995
	Fuel-Fraction (Climb)	$M_{ff,CLB}$	0.985
	Fuel-Fraction (Descent)	$M_{ff,DES}$	0.985
	Fuel-Fraction (Landing)	$M_{ff,L}$	0.995
General	Operating empty mass ratio	m_{OE}/m_{MTO}	0.579
	Passenger mass with luggage (short/ medium haul)	m_{PAX}	93 kg
	Number of passengers	n_{PAX}	180
	Cargo mass	m_{cargo}	1230 kg

Table B.3 Input data Excel tool diesel aircraft (500 NM)

Segment/ Category	Parameter	Abbreviation	Value
Approach/ Landing	Approach factor	K_{APP}	1.939
	Safety landing distance	S_{LFL}	1550 m
	Mass ratio landing/take-off	m_{ML}/m_{MTO}	0.932
	Wing loading at take-off mass	m_{ML}/S_W	636.15 kg/m ²
Take-off	Safety start distance	S_{TOFL}	2090 m
	Start temperature above ISA (288.15K)	ΔT_{TO}	0 K
	Density ratio	σ	1
	Take-off factor	k_{TO}	2.25
	Propeller disc diameter	d_{disc}	5.30 m
	Take-off power of one engine (reference)	$P_{S,TO}/n_E$	8251000 W
	Propeller efficiency	η_P	0.65
2nd Segment	Aspect ratio	A	9.485
	Zero drag coefficient (clean)	$C_{D,0}$	0.02
	Zero drag coefficient (slats)	$\Delta C_{D,slat}$	0
	Oswald factor; with flap deflection	e	0.75
	Number of engines	n_E	4
	Propeller efficiency	η_P	0.65
Missed Approach	Zero drag coefficient (clean)	$C_{D,0}$	0.02
	Zero drag coefficient (slats)	$\Delta C_{D,slat}$	0
	Zero drag coefficient (undercarriage)	$\Delta C_{D,UC}$	0.015
	Propeller efficiency	η_P	0.64
Cruise	Max. glide ratio	E_{max}	18
	Oswald factor (clean)	e	0.85
	Mach number (Cruise)	M_{CR}	0.68
	Propeller efficiency	η_P	0.85
		V/V_{md}	0.910
	Design range	R	500 NM
	Flight distance to alternate airport	$S_{TO,alternate}$	200 NM
	FAR Part 21-Reserves: international		
Specific fuel consumption	C_{CR}	$5.8 \cdot 10^{-8}$ kg/W/s	
Fuel Fraction	Fuel-Fraction (engine start)	$M_{ff,E}$	0.990
	Fuel-Fraction (Taxi)	$M_{ff,T}$	0.995
	Fuel-Fraction, (Take-Off)	$M_{ff,TO}$	0.995
	Fuel-Fraction (Climb)	$M_{ff,CLB}$	0.985
	Fuel-Fraction (Descent)	$M_{ff,DES}$	0.985
	Fuel-Fraction (Landing)	$M_{ff,L}$	0.995
General	Operating empty mass ratio	m_{OE}/m_{MTO}	0.662
	Passenger mass with luggage (short/ medium haul)	m_{PAX}	93 kg
	Number of passengers	n_{PAX}	180
	Cargo mass	m_{cargo}	1230 kg